

INTERACTIONS OF ORTHOPHOSPHATE WITH
IRON OXYHYDROXIDE MINERALS FOUND IN SOILS

BY

BOURAHIM YEKINI

A DISSERTATION PRESENTED TO THE GRADUATE COUNCIL OF THE
UNIVERSITY OF FLORIDA
IN PARTIAL FULFILLMENT OF THE REQUIREMENTS FOR THE DEGREE OF
DOCTOR OF PHILOSOPHY

UNIVERSITY OF FLORIDA

1980

J M15 80 2174

To
The African People

ACKNOWLEDGEMENTS

The author wishes to express his sincere appreciation to Dr. John G. A. Fiskell, chairman of the supervisory committee, for his guidance and assistance throughout the entire course of this study, and for his valuable suggestions and excellent assistance in the preparation of this manuscript. The author is pleased to extend his sincere acknowledgements to Dr. J. J. Street and Dr. V. E. Berkheiser for their participation in the supervisory committee and constructive criticism of this manuscript.

Appreciations are also extended to Dr. W. K. Robertson, Dr. R. C. Stoufer and Dr. T. L. Yuan for various assistances.

Special recognition is expressed to Dr. Charles F. Eno, chairman, Soil Science Department, Dr. B. G. Volk, and Dr. D. F. Rothwell.

Sincere appreciation is expressed to the African-American Institute which sponsored this study.

Appreciations are also extended to Carol Giles for her excellence in typing.

The author wishes to express the deepest gratitude to his mother Mariama, his wife Olga and daughter Maryam, and his brothers and sisters for their moral support.

TABLE OF CONTENTS

	<u>Page</u>
ACKNOWLEDGEMENTS	iii
ABSTRACT	xi
INTRODUCTION	1
CHAPTER	
I	REVIEW OF SOME MODELS DESCRIBING FACTORS
	AFFECTING NUTRIENT AVAILABILITY 4
	Nutrient Potential 4
	Capacity and Intensity Relationship 7
	Energy of Adsorption 8
	Some Adsorption Isotherm Models 10
	Effect of Surface Heterogeneity
	on Adsorption-Desorption 12
	Generalization of Adsorption
	Isotherms 14
	Soil Phosphorus Reaction Mechanisms 16
	Specific Adsorption 19
	Infrared Study of Phosphate Specific
	Adsorption 21
II	KINETICS OF ADSORPTION AND DESORPTION 26
	Adsorption 26
	Desorption 27
	Adsorption and Desorption Relationships 27
	A Kinetic Model for Adsorption-Desorption 28
III	THERMODYNAMICS OF ADSORPTION-
	DESORPTION REACTION 33
	The Surface Charge 33
	Zero Point of Charge (ZPC) 35
	Thermodynamics of Adsorption 36
	Free Energy as a Function of Distance 36
	Free Energy for Irreversible Fixation 38
	Relationship of Surface Charge to
	Surface Potential 39
	Surface Tension and Specific Adsorption 40

TABLE OF CONTENTS
(Continued)

CHAPTER		<u>Page</u>
IV	MATERIALS AND METHODS	41
	Goethite Preparation	41
	Some Factors Affecting the Kinetics of Adsorption-Desorption	42
	Surface Charge as Affected by Phos- phate Adsorption	45
	Soil pH, Iron Oxides, and Extractable P	46
V	RESULTS AND DISCUSSION	48
	Goethite and Phosphated Goethite Study by Infrared Spectroscopy	48
	Goethite Structure Identification by Infrared	49
	Factors Affecting Goethite Crystallization	60
	Phosphate Adsorption and Desorption Studies	69
	Effect of the Supporting Electrolyte	77
	Time of Reaction Effects	88
	Effects of pH on P Adsorption and Desorption	99
	Effects of P Adsorption on Surface Charge of Goethite	108
VI	SUMMARY AND CONCLUSION	112
	LITERATURE CITED	118
	BIOGRAPHICAL SKETCH	123

LIST OF TABLES

<u>Table</u>		<u>Page</u>
1	Soil pH, iron oxide, and extractable P	47
2	Type of salt effect on the P adsorption on goethite at 5 mg P/ml	79
3	Effects of three electrolyte salts on the phosphate sorption maximum and sorption energy constant for goethite	81
4	Phosphate desorption from goethite by different anions	85
5	Effect of reaction time on phosphate adsorption maximum and sorption energy constant for the goethite system	85
6	The logarithm of (a) equilibrium P con- centration as a function of the logarithm of (b) the amount P adsorbed	85
7	Effects of P adsorption on the equilib- rium solution pH after 24 hours of adsorption reaction	101

LIST OF FIGURES

<u>Figure</u>		<u>Page</u>
1	Schematic representation of solid-interface-solution system	29
2	Infrared bands of (A) goethite; (B) phosphate added to goethite at the end of ageing; and (C) phosphate added to goethite at beginning of ageing. Curves A, B and C are for 22°C and curves A', B' and C' are for 55°C	50
3	Infrared bands of (A) goethite; (B) phosphate added to goethite at end of ageing; and (C) phosphate added to goethite at beginning of ageing. Curves A, B and C are for 22°C and curves A', B' and C' are for 55°C	51
4	Infrared bands of (A) goethite; (B) phosphate added to goethite at end of ageing; and (C) phosphate added to goethite at beginning of ageing. Curves A, B and C are for 22°C and curves A', B' and C' are for 55°C	54
5	Infrared bands of goethite and lepidocrocite. (After Farmer and Palmieri 1975)	55
6	Infrared bands of (A) goethite; (B) phosphate added to goethite at end ageing; and (C) phosphate added to goethite at beginning ageing. Curves A, B and C are for 22°C and curves A', B' and C' are for 55°C	56
7	Infrared bands of (A) Fe hydroxide material; (B) phosphate added to Fe hydroxide material at end ageing; and (C) phosphate added to Fe Hydroxide material at beginning ageing. Curves A, B and C are for 22°C and curves A', B' and C' are for 55°C	57

LIST OF FIGURES
(Continued)

<u>Figure</u>		<u>Page</u>
8	X-ray diffraction patterns of (A) goethite, (B) phosphated goethite at end of ageing, and (C) phosphated goethite at beginning of ageing	59
9	Infrared bands of phosphated goethite at beginning of ageing for suspensions of various P/Fe values at OH/Fe = 6	62
10	Infrared bands of phosphated goethite at beginning of ageing for various P/Fe ratios at OH/Fe = 3.0	63
11	Infrared bands of phosphated goethite at beginning of ageing for various P/Fe ratios at OH/Fe = 1.5	64
12	Infrared bands of 1) goethite digested in D ₂ O and 2) phosphated goethite digested in D ₂ O	66
13	Infrared band of phosphated goethite after desorption by (1) 0.1 N KCl, (2) H ₂ O, (3) 0.1 N KNO ₃ , and (4) 0.1 N Na ₂ SO ₄	67
14	The 001 face of goethite lattice. (After Bragg and Claringbul 1965)	69
15	The 001 face of phosphated goethite	69
16	Adsorption isotherms as affected by the reaction times for goethite-solution systems	71
17	Adsorption isotherm for the Kenya soil after 24 hours of reaction time	72
18	Adsorption isotherm for the Georgia soil after a reaction time of 24 hours	73
19	Phosphate adsorption isotherm for the Colorado soil after 24 hours of reaction time	74

LIST OF FIGURES
(Continued)

<u>Figure</u>		<u>Page</u>
20	Effects of the initial P concentration on the phosphate adsorption by goethite-solution (1 g/1000 ml)	76
21	Effects of the type of supporting electrolyte on P adsorption on goethite suspension (1 g/1000 ml)	78
22	Effects of the supporting electrolyte concentration on the kinetics of P adsorption by the goethite-solution system (1 g/1000 ml)	84
23	Phosphate desorption in 10 hours from goethite by three salt solutions at various equilibrium P concentration	87
24	Transformed Langmuir equations for phosphate sorption by goethite as affected by reaction times. a is equilibrium concentration and b amount adsorbed	80
25	Change in the equilibrium P concentration and P sorption as affected by the reaction time	89
26	Change in the equilibrium P concentration for three soils as affected by the reaction times	90
27	Effect of reaction time and equilibrium P concentration on P desorbed by 0.01 N CaCl_2 from Kenya soil	95
28	Effect of reaction time and equilibrium P concentration on P desorbed by 0.01 N CaCl_2 from Georgia and Colorado soils	97
29	Effect on P desorbed by 0.5 N NH_4F as affected by the adsorption reaction time and equilibrium P concentration	98

LIST OF FIGURE
(Continued)

<u>Figure</u>		<u>Page</u>
30	Logarithmic plot of equilibrium P concentration change with time (t) relative to equilibrium at 18 hours (t_0) for phosphated goethite	93
31	Effects of change in equilibrium solution pH on P adsorption and 0.01 N CaCl_2 desorption of P in goethite system. Initial P concentration is 5 $\mu\text{g P/ml}$	100
32	Effect of phosphate adsorption time on phosphate desorption by 0.01 N CaCl_2 at pH 2 and pH 10	104
33	Effects of solution pH on the amount of P desorbed from goethite	106
34	Effects of pH and concentration of supporting electrolyte on phosphate desorption	107
35	Potentiometric titration of goethite. Note zero point of charge occurs at pH 5.8	109
36	Potentiometric titration of phosphated goethite. Note zero point of charge occurs at pH 5.2	110

Abstract of Dissertation Presented to the Graduate Council
of the University of Florida in Partial Fulfillment of the
Requirements for the Degree of Doctor of Philosophy

INTERACTIONS OF ORTHOPHOSPHATE WITH
IRON OXYHYDROXIDE MINERALS FOUND IN SOILS

By

Bourahim Yekini

June 1980

Chairman: Dr. John G. A. Fiskell
Major Department: Soil Science

The mechanisms, kinetics, and reversibility of orthophosphate adsorption on synthetic goethite and soils were investigated. Goethite was prepared by ageing of the precipitate which appears after mixing FeCl_2 and NaOH solutions. Both the increase in Fe/OH ratio in the suspension and in ageing temperature favored a higher degree of goethite crystallization within a short period of time. With either $\text{OH}/\text{Fe} = 6$ in the suspension at room temperature or $\text{OH}/\text{Fe} = 3$ at 55°C and ageing for one week, good goethite yield was obtained. Infrared bands characteristic of goethite were at 3200 cm^{-1} (OH stretching) and at 890 cm^{-1} and 790 cm^{-1} (both are $\text{Fe}-\text{OH}$ bending vibration). The goethite structure was confirmed by X-ray diffraction intensities of the 4.19 \AA and 2.70 \AA peaks. The presence of phosphate at the beginning of goethite ageing weakened the goethite structure. When $\text{P}/\text{Fe} = 3.2$ (regardless of OH/Fe ratio) the bond $(\text{Fe})-\text{O}-\text{P}$ vibration at 1000 cm^{-1} was predominant, thus preventing the formation

of Fe-OH bond even after ageing of a suspension. When the addition of phosphate was made at the end of the goethite ageing, absorption of phosphate was determined as surface binding through binuclear bridging of the HPO_4^{2-} ion which was identified by the presence of bands at 1120, 1085, and 1030 cm^{-1} . The phosphate was assumed to penetrate the goethite structure whenever the vibrational band at 1000 cm^{-1} was present.

Using synthetic goethite as supporting medium, it was found that the Langmuir and Freundlich equations could be used to describe the relation between the amount of P adsorbed and that remaining in the equilibrium solution for particular periods of reaction time.

A kinetic model was proposed to describe the change with time of each of the following ion forms: 1) the free ions in solution, 2) the physically adsorbed, 3) the reversible chemically adsorbed ions, and 4) the irreversible chemically adsorbed ions. The amount of phosphate adsorbed increased with the increase in initial P concentration and the adsorption reaction time. The time required for the goethite phosphate system to reach an equilibrium state increased with the initial P concentration. Generally, the equilibrium state was reached after 18 hours for goethite-solution and 22 hours for soil-solution systems. The adsorption on goethite was increased by both multivalent cations

and the concentration of the supporting electrolyte. The potential binding energy constant increased (from 0.70 to 4.60 ml/ μ g P) as the reaction time increased, but decreased as the cation valence of the electrolyte was increased.

At the same initial P concentration, the amount of P adsorbed decreased almost linearly with change in pH according to the relation μ g P/g goethite = $-446 \text{ pH} + 5680$. The amount of P desorbed over a wide range pH or supporting electrolyte remained nearly constant when the desorbing time was greater than or equal to 6 hours. The P desorbed from goethite and/or soils increased both with the initial equilibrium P concentration employed and the reaction time. At the same initial P adsorbed on goethite, the amount of P desorbed from goethite decreased when the pH was below 5.5 and increased when the pH was greater than 6. Phosphate adsorption on goethite was found to induce a net increase of negative charge so that the zero point of charge declined from pH 5.8 to 5.2.

INTRODUCTION

Increase in urbanization makes it necessary to increase both the quantity and the quality of agricultural production in the tropical region. The implementation of an adequate agricultural policy involves improvements of the actual level of technology. This implies a clear understanding that the macroscopic relation be sought between the major factors producing food for human population through proper managements of soils, plants, animals, and insects under diverse climates and social activities. Modeling of the agricultural system is a useful tool for understanding a united approach for all major factors governing the system. With a suitable model, it should be possible to envisage needed change in a particular factor in order to give results as close as possible to a reasonable expectation. Only some microscopic relationships within the soils will retain our attention in this study. In a soil-solution system, the dominant soil phenomena taking place simultaneously are mass transport, diffusion, adsorption-desorption, precipitation-dissolution, and microbial immobilization and mineralization. The dominance of each soil phenomenon depends on the soil structure and texture, organic matter content, water content, temperature, and the ionic suite (types and concentrations).

Upon fertilization, tropical soils may not react in the same way as do the temperate soils because of their different mineralogical, and chemical properties. Among the major elements, phosphorus is, after nitrogen, the most deficient nutrient and its availability is strongly dependent on the mineralogical composition of the soil (type of clay, and metal oxides). The low availability of phosphate to tropical plants is due both to the high soil phosphate fixing capacity and to precipitation of fertilizer phosphorus from the soil solution. Not all forms of phosphorus bound on the oxide surfaces are held with the same degree of strength. With time, as phosphorus is depleted from the solution, some phosphate may be replenished by release from the solid phase. The magnitude of this release, with respect to time, is dependent on soil characteristics. The initial concentration in solution is not a sufficient measure of phosphorus availability. In tropical soils, iron oxides are quite important in determining the solid phase capacity to fix and supply phosphorus to the soil solution. How some factors, such as OH/Fe ratio, temperature, and phosphate concentration affect the formation of goethite are herein investigated. Infrared spectroscopy will be used to identify the effects of soluble phosphate on goethite structure and the nature of phosphate binding on goethite. Synthetic goethite as well as three soils will be used to investigate some

factors affecting the time dependance and the degree of reversibility of orthophosphate adsorption.

CHAPTER I
REVIEW OF SOME MODELS DESCRIBING FACTORS
AFFECTING NUTRIENT AVAILABILITY

Nutrient Potential

The concept that availability of a nutrient can be described by its potential activity was first brought to general notice by Schofield (1955). His concept was that in comparing two soils of different water holding capacity which contain the same amount of available water, the one having the lower capacity has a lower potential and the water is easier to extract than from the soil of higher holding capacity. Their pF value defines the energy with which water is held on the soil particle surface. The potential given by the pF value provides the basis for quantitative evaluation of the availability of water. As water is taken out of a soil, it is replaced by lateral movement of groundwater. Similarly, as a nutrient is taken from the soil solution, it is replaced by other ions, by desorption, or by diffusion as well as mass flow. Eventually, it is not the amount of a nutrient in a soil that primarily controls the uptake of that nutrient by the plant, but the work required to withdraw it from the solution. This work may be related to Gibb's free energy (G_1) if the uptake is mainly from the soil solution. To derive an expression for

the nutrient potential, three postulates have been advanced by different workers.

Postulate 1

Where the solution is at constant temperature and pressure, and when the system is at equilibrium, G_i is uniform throughout the soil solution so that

$$G_i = G_i^O + RT \ln a_i^f + zF\psi_i^f \quad (1)$$

where G_i^O is the standard molar free energy of an ion i in the solution relative to an arbitrarily zero of the electric potential, a_i^f is the activity of this ion in solution, z is the valence, F is the Faraday constant, and ψ_i^f is the electric field effects.

Postulate 2

When a soil is in equilibrium with a solution, the electro-chemical potential of the ion is constant throughout the system (soil-solution). Then, the partial molar free energy of any ion in the soil complex can be determined by analyzing the solution. This free energy of the ion in solution is assumed to be constant even if the solution is separated from the solid phase by centrifugation. As a result, if the ion is taken out of the field influence, then $zF\psi = 0$ where z , F , and ψ are as described in the previous section. Then the relationship in Eq. (1) can be reduced to

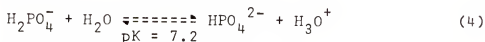
$$G_i = G_i^O + RT \ln a_i^f \quad (2)$$

Postulate 3

This postulate is that potentials are determined by transfers of ions. In order to maintain the electroneutrality, equal transfer must occur for quantities of positive and negative ions in one direction or, alternatively, transfer of one ion in the first direction occurs as an equivalent quantity of ions of the same sign moves in the opposite direction (Barrow et al. 1965). It is also assumed that divalent cations (Ca and Mg) dominate most soil surfaces as exchangeable cations and in the solution, except for saline soils. For a situation in which transfer of Ca^{2+} is in one direction and K^+ in the other, the net change in free energy is

$$\Delta G_{\text{Ca,K}} = \Delta G_{\text{Ca,K}}^O + RT(\ln a_K - \ln a_{\text{Ca}}) \quad (3)$$

For phosphorus, over the range of pH which exists in soil, two forms of the orthophosphate ions are in equilibrium; thus



Assuming that plants absorb mainly H_2PO_4^- ion and not HPO_4^{2-} , then a cation such as Ca^{2+} must accompany the H_2PO_4^- . The equation for the transfer of both ions from the equilibrium solution is

$$\Delta G_{\text{Ca}(\text{H}_2\text{PO}_4)_2} = -2.3 RT(1/2p\text{Ca} + p\text{H}_2\text{PO}_4) \quad (5)$$

A common use of the relationship is the Schofield's phosphorus potential, where I is given by $I = 1/2 \text{Ca}^{2+} + p\text{H}_2\text{PO}_4$.

Capacity and Intensity Relationship

Phosphorus ions pass from one phase to another as a result of chemical potential differences between the phases. In general, any substance tends to pass from a region of higher chemical potential to a lower one. The ability of the solid phase to supply phosphorus to the solution phase, as it is depleted, can be termed the capacity. For any ion such as phosphorus, at equilibrium, the phosphorus buffering capacity (PBC) is a soil characteristic where $\text{PBC} = d\Delta P/dI$. The term with $I = 1/2p\text{Ca}^{2+} + p\text{H}_2\text{PO}_4^-$ and ΔP is the gain or loss in phosphorus by the soil. The relationship between capacity and intensity factors is expressed as Q/I curves which are generally composed of two parts with linear and curvilinear portions. In the Q/I relationship for potassium, the curved portion is attributed to a number of sites which have specific affinity for potassium at low concentration and the linear part is associated to non-specific sites, Beckett (1971). He also believed that, in general, the curved part of the Q/I relation can be represented by a Langmuir adsorption isotherm whereas the linear part fits the Gapon relationship.

Beckett (1971) affirmed that the non-linear part of the curve represents a certain region where there is a definite and limited number of sites on the exchangeable surfaces and exhibits a selective binding power for the adsorbing ion: The Langmuir adsorption isotherm could be used to describe such a situation. In addition, if Eq. (3) is recalled, the activity ratio (AR) is $K^+/(Ca)^{1/2}$ of the ions in solution which is the product of the concentration of the exchangeable ions and the Gapon constant (k_G).

Energy of Adsorption

Partition Function

To be effective, the collision between molecules and the collision surface must provide a certain minimum amount of energy called the activation energy. Since the activated complex is a transitory species, the equilibrium constant cannot be measured experimentally. However, the partition function arises from the quantum theory that a molecule can exist only in states with definite energy limits. From Boltzman distribution, it is recognized that

$$N_A = N_{OA} / g_{OA} \sum g_{iA} \exp(-E_{iA}/kT) \quad (6)$$

where N_A is the total number of molecules, N_{OA} is the number of molecules at zero energy, E_{iA} is the activation energy at the state i , and g_i is a constant. In this case, also quantity $Q = \sum g_{iA} \exp(-E_{iA}/kT)$ which is the partition function.

Electric Field Effect

The following treatment was first derived for solid-gas interaction and is known as Thin's theory reported by Brunauer (1943). The strength of the electric field surrounding the adsorbent is given by $E = e_1/\epsilon r_0$, where e_1 is the charge distribution of the adsorbent, ϵ is the dielectric constant of the gas, and r is the distance from the surface.

The force (F) acting on an induced dipole is

$$F = k e_1^2 v / 4 n r^{2v+1}$$

where v is a constant and $k = \epsilon - 1/\epsilon$. The adsorption potential is the force multiplied by the distance through which it acts ($F \cdot \Delta r$).

Heat of Adsorption

Assuming no work due to phase change is done during the adsorption-desorption, the molar energy of the ion in free solution (u_A) and the energy of the ion in the adsorbed phase (u_B) are related to the loss of ion from the solution due to adsorption as shown by

$$\Delta H = b(u_A - u_B) \quad (7)$$

where b is the number of mole adsorbed, and ΔH is the integral heat of adsorption.

Differential Heat of Adsorption

Assuming that the adsorption process is reversible ΔH can be obtained from data at two temperatures (T_1 and T_2) by

using the Clausius-Clapeyron equation for a constant surface coverage, namely

$$\ln \left[\frac{a_2}{a_1} \right] = \frac{\Delta H}{R} \left[\frac{1}{T_1} - \frac{1}{T_2} \right] \quad (8)$$

where a_1 and a_2 are equilibrium concentrations at temperature T_1 and T_2 , respectively, and R is the molar gas constant.

Some Adsorption Isotherm Models

Freundlich Equation

The Freundlich equation was first introduced in an empirical form (Bach and Williams 1971). It assumed that the energy of adsorption decreases exponentially with increasing saturation of the surface. The equation is

$$b/m = ka^{1/n} \quad (9)$$

where b/m is the amount of phosphorus adsorbed per unit weight of soil at the equilibrium concentration termed a , and where k and n are constants. The logarithmic form of Eq. (9) is

$$\log(b/m) = \log k + 1/n \log a \quad (10)$$

The plot of $\log(b/m)$ versus $\log a$ should yield a straight line. This equation is valid only in a limited range of concentrations. By taking into account the initially exchangeable phosphorus and the ability of the soil to lose or gain phosphorus (ΔP) during the equilibrium reaction, the following modification was introduced

$$\Delta P = \Delta a = ka^{1/n} - e \quad (11)$$

where Δa is the amount of phosphorus gained or lost, e is the phosphorus initially present, and n is a constant.

Modified Freundlich Equation

In a colloid-solution system, the adsorption is time-dependent. Kuo and Lotse (1972) introduced a time factor $1 - e^{-k_2 t}$ after assuming that the constant k_2 is small. They found that

$$b/m = k a_0 t^{1/n} \quad (12)$$

where a_0 is the initial phosphorus concentration. Their study indicated that the rate constant increased with an increase in concentration.

Langmuir Equation

The derivation of the Langmuir equation is based on the following assumptions: 1) the energy of adsorption is constant and independent of the degree of coverage, 2) there is not interaction between adjacent adsorbed molecules on an homogenous surface. If the system is in dynamic equilibrium, this results when the rate of adsorption is equal to the rate of molecules escaping from sorption surface, so that

$$k_1 \theta = k_2 P(1 - \theta) \quad (13)$$

where k_1 and k_2 are the rate constants of adsorption and desorption, P is the gas pressure, and θ is the fraction of the surface coverage by the gas. By rearrangement, the relationship is

$$\theta = \frac{ksP}{1 + kP} \quad (14a)$$

and by analogy

$$\theta = \frac{k_s a}{1 + k_a a} \quad (14b)$$

for soil-solution system, where a is the ion concentration in solution. The above equation can be put in the linear form as follows

$$a/b/m = a/s + 1/ks \quad (14c)$$

where k is the adsorption energy constant and s is the adsorption maximum. Different workers have observed that there is not a linearity between $a/b/m$ and a . This may be caused by at least two types of sites of adsorption having different energies of adsorption. To fit this criterion, the Langmuir equation was modified to be

$$\theta = \frac{k_1 s_1 a}{1 + k_1 a} + \frac{k_2 s_2 a}{1 + k_2 a} \quad (14d)$$

where k_1 , s_1 are constants for region 1, and k_2 , s_2 are constants for region 2 (Syers et al. 1973).

Effect of Surface Heterogeneity on Adsorption-Desorption

Langmuir and Freundlich equations can be obtained from Toth's equation (Jossen et al. 1978), for homogeneous surface. Toth's equation is obtained by integrating the equation

$$\psi = \frac{d \ln a}{d \ln b} - 1 = \alpha a^\beta \quad (15)$$

Where $\beta = 0$, the Freundlich equation is obtained. Where $\beta = 1$, the Langmuir type of equation is

$$b = \frac{b^{\infty} a}{\delta + a} \quad (16)$$

where $\delta = d \exp(-E/RT)$, a is the equilibrium concentration, b the amount adsorbed and b^{∞} is the maximum adsorption.

Another factor is that the energy of activation (E) is constant for a homogeneous surface but varies on a heterogeneous surface with the degree of coverage (Jossen et al. 1978). Assuming that the free energy of activation for adsorption varies linearly with coverage of the surface, Lingstrom et al. (1970) proposed the following model



where A is the adsorbate, S is the surface, and k_1 and k_2 are the rate constants. They deduced that the rate of adsorption process is

$$d\theta/dt = k_1(1-\theta)(1-1/2\theta)e^{-b\theta} + k_2[(1-1/2\theta)e^{-b(2-\theta)} - 1/2\theta^2 e^{b\theta}] \quad (18)$$

where $\theta = b/b^{\infty}$.

Another useful relationship is the Elovich equation where the activation energy is a linear function of the amount adsorbed

$$E = E_0 + \alpha b \quad (19a)$$

Aharoni and Ungarish (1977) modified this equation by introducing the fact that the heterogeneous surface is comprised of a large number of homogeneous regions having unequal number of adsorption sites.

$$E_t = E_o + RT \ln(g y_t / n_E + \gamma) \quad (19b)$$

where $y_t = db/dE$, g and γ are constant, and n_E is the number of sites of energy E_t , where E_t is the activation energy characteristic of a region. They also assumed that, at any moment, adsorption takes place preferentially on the region that has the lowest activation energy at that moment.

Considering the case where equilibrium is attained at a region when $y_t = y_{eq}$, then it follows that $y_{eq} = k_c \exp(E/RT)$. The overall rate of adsorption is given by

$$db/dt = k_o N_t \exp(-E_t/RT) \text{ and } N_t = \int n_E dE \quad (20)$$

where N_t is the number of sites with an energy E_t at time t and n_E is the number of sites with an activation energy between E and $E + dE$.

Generalization of Adsorption Isotherms

Freundlich and Langmuir equations can be extended for cases of competitive adsorption (Jaroniec and Toth 1976; Digiani et al. 1978). In this case, the Freundlich type is given by

$$b_1 = k(\sum_i a_i) \quad (21)$$

and the Langmuir type by

$$b_1 = k a_1 / (k_o + k_1 a_1 + k_2 a_2 + \dots + k_i a_i) \quad (22)$$

which is a partial isotherm of a_1 relative to the total ions present. A binary system can be simplified if the following

assumptions are made, 1) the surface is formed by a collection of regions each being characterized by a binding energy (E), 2) the number of surface atoms N_i with energy E follow the Boltzman distribution, which is described by

$$N_i = N_0 \exp(-\epsilon/RT) \quad (23a)$$

and 3) all adsorbed molecules stay on the surface for the same average length of time δ so that

$$\delta = \delta_0 \exp(E/RT) \quad (23b)$$

During the time δ , the fluctuation of the number of adsorbed and desorbed molecules compensate between themselves randomly (Vlad and Segal 1979). They considered that the adsorption energy is an increasing function of the extra energy ϵ .

From McLaurin development, the extra energy can be expressed as

$$\epsilon = \sum_n \alpha_n (E - E_m)^n \quad (24)$$

where E_m is the smallest adsorption energy corresponding to the value of zero energy and n is generally integers of 1 or 2.

The energy distribution $X(\epsilon)$ is expressed by Van Dongen approximation as

$$X(\epsilon) = \exp\left(\sum_i a_i \epsilon\right) \quad i = 0, 1, \text{ or } 2. \quad (25a)$$

or generally as

$$X(\epsilon) = \frac{1}{kT} \sum_{n=1}^N n \alpha_n (E - E_m)^{n-1} \exp[-1/kT \sum_{n=1}^N \alpha_n (E - E_m)^n] \quad (25b)$$

The general isotherm is expressed as

$$b(a,T) = \int_{\Omega} b_1(a,\epsilon) X(\epsilon) d\epsilon \quad (26)$$

where $b(a,T)$ is the fraction of the total surface covered at (a,ϵ) , $b_1(a,\epsilon)$ is the local isotherm which may be analogous to an isotherm equation for an homogeneous surface or region, Ω is the range of possible variation of adsorption energy assuming that $\Omega = [0,\infty]$.

Temperature Dependence of the Rate Constant

According to the Arrhenius equation, it is known that

$$k_{\text{ads}} = A \exp(-E_a/RT) \quad (27a)$$

where E_a is the energy of activation, R is the gas constant, and T is the absolute temperature.

From the transition state theory, this relationship is extended to

$$k_{\text{ads}} = (kT/h) \exp(\Delta S_a/R) \exp(-\Delta H_a/RT) \quad (27b)$$

$$= (kT/h) \exp(\Delta G_a/RT) \quad (27c)$$

where ΔS_a is the entropy of activation, $\Delta H = E_a - RT$ which is the enthalpy of activation, and ΔG_a is the Gibb's free energy of activation.

Soil Phosphorus Reaction Mechanisms

Plant responses to soil phosphorus are a function of the solubility of phosphorus. Any factor altering the solubility of phosphorus will also alter the plant response

(Hemwall 1957). The solubility of phosphorus depends on several factors such as the composition of the soil solution, the pH of the solution, and temperature of the soil-solution system.

Calcareous and Neutral Soils

The adsorption of phosphorus on calcareous surfaces can take place by replacement of water molecules, bicarbonate, and certain other anions or cations. The relative strength of the phosphate ion adsorption depends on the solubility of the compound at the calcium surface (Kuo and Lotse 1972).

The precipitation of phosphorus may be due to the formation of a whole series of insoluble calcium phosphates. Some of these with associated solubility products expressed as the pK value are reported by Lindsay and Moreno (1960).

<u>Compounds</u>	<u>Chemical formula</u>	<u>pK</u>
Calcium phosphate anhydride	CaHPO_4	6.66
Calcium phosphate dihydrate	$\text{CaHPO}_4 \cdot 2\text{H}_2\text{O}$	6.56
Octocalcium phosphate	$\text{Ca}_4\text{H}(\text{PO}_4)_3 \cdot 3\text{H}_2\text{O}$	46.91
Hydroxyapatite	$\text{Ca}_{10}(\text{PO}_4)_6 \cdot (\text{OH})_2$	113.70
Fluorapatite	$\text{Ca}_{10}(\text{PO}_4)_6 \cdot \text{F}_2$	118.40

In calcareous soil, hydroxyapatite and fluorapatite are the major phosphorus compounds, whereas in neutral soil, octocalcium phosphate becomes important and in moderately acidic soils dicalcium phosphate may occur.

Acid Soils

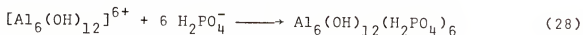
Iron, aluminum and pH are the main factors controlling phosphorus solubilities: In acid soils, the solubility of phosphorus increases with decreasing free iron and aluminum activities and with increasing pH. The form of phosphate sorbed by acidic soils was recovered (90%) as iron and aluminum phosphates (Ghani and Islam, 1946). Yuan et al. (1960) reported that up to 80% of the added phosphorus to acid sandy soils was present as aluminum phosphate and 10% as iron phosphate, but when the reaction temperature was increased more iron phosphate was formed.

After reaction of phosphorus with soluble Al^{3+} , a microscopic examination showed an hexagonally shaped crystal in which the interplanar spacing was similar to those of palmerite (Haseman et al. 1950). In general, some of the main forms in which phosphorus can precipitate with iron and aluminum are given below.

<u>Compounds</u>	<u>Chemical formula</u>	<u>pK</u>
Variscite	$AlPO_4 \cdot 2H_2O$	30.5
Strengite	$FePO_4 \cdot 2H_2O$	34.3
Taranakite	$(K, NH_4)_3H_6Al_5(PO_4)_8 \cdot 18H_2O$	176.0
Palmerite	$HK_2Al_2(PO_4)_3 \cdot 7H_2O$	

Since Al and Fe atoms are part of the surface colloids, they react with phosphates. Whether the process is

precipitation or adsorption depends on the size of the metal polymer and the pH of the phosphate, and its concentration. In a moderately acidic medium, with a high phosphorus concentration, the reaction process may be typically precipitation, resembling that reported by Hsu (1965),



Specific Adsorption

General Description

In a solid-solution system, adsorption of molecules (or ions) occurs when there is a change in phase from the free state (in solution) to the bound state at the interface. Ions deposited at the surface likely orient to form the Stern layer as some ions may approach closely to the surface structure. In this case, the ions are said to be specifically adsorbed on the surface.

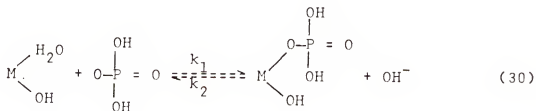
Non-specifically adsorbed ions are either in the diffuse Gouy-Chapman region separated from the solid surface by at least one molecule, or electrostatically bound to that surface. Specifically adsorbed ions are in the coordination shell of the surface atoms and are maintained there through chemical binding (covalent or coordinate binding). Since specific adsorption of cations or anions occurs even when the surface possesses a net positive or negative charge, respectively, there must be an electrostatic contribution due to polarization of the ion or molecule.

Both chemical and electrostatic attractions contribute to the energy of adsorption. The magnitude of this energy of adsorption determines the degree of reversibility and the amount adsorbed. Since the reaction is pH dependent, at any pH, there is a maximum adsorption of anions and when these maxima are plotted against pH, the curve is termed the adsorption envelope which is described by Hingston et al. (1967) as

$$A = 2V\sqrt{(1 - \alpha)} = 2V\sqrt{\frac{K[H]}{(K + [H])^2}} \quad (29)$$

where A is the amount of the ion adsorbed per unit weight of adsorption, α is the degree of dissociation of acid anion, K is the dissociation constant of the most highly charged anion that is adsorbed, and V is the amount of ion adsorbed at the maximum level.

Why some of the adsorbed anions such as phosphate may be irreversibly held is explained by certain postulated mechanisms of phosphate adsorption. The removal of phosphate from free solution is assumed to proceed through the replacement of coordinated H_2O groups and/or some OH^- ions,



where M is a metal (Fe or Al), and bonded by a coordination link.

Infra-red Study of Phosphate Specific Adsorption

Theory of Infra-Red Spectroscopy

If a molecule is placed in an electromagnetic field, a transfer of energy from the field to the molecule occurs when Bohr's frequency condition is satisfied: $\Delta E = h\nu$, where ΔE is the difference in energy between two quantized states, h is Plank's constant, and ν is the frequency of the light wave. Pure rotational vibrations are usually observed in the microwave vibrational spectra in the infrared whereas electronic spectra are in the visible and ultraviolet. The infrared spectra originate in the transition state existing between two vibrational levels of the molecules. From a classical point of view, a vibration is active in the infra-red spectrum if the dipole moment of the molecule is changed during the vibration. The dipole moment Q is related to the strength of the electric field by $Q = \alpha E$ and Q is a vector whose direction is the line between the center of gravity of the protons and electrons. Let a diatomic molecule be represented by two masses m_1 and m_2 moving along the molecule's axis with displacements of X_1 and X_2 respectively. The displacements of the two atoms are induced by forces which can be obtained through Hooke's and Newton's law.

$$K(X_2 - X_1) = m_1 \frac{d^2 X_1}{dt^2} \text{ and } -K(X_2 - X_1) = m_2 \frac{d^2 X_2}{dt^2} \quad (31)$$

The solutions of these equations of motion are:

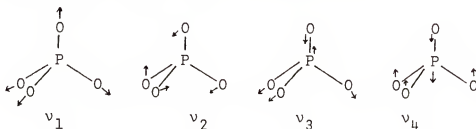
$$X_1 = A \cos(2\pi \nu t + \alpha) \text{ and } X_2 = A \cos(2\pi \nu t + \alpha) \quad (31b)$$

After differentiating and substituting back in Eq. (31), it can be found when solving for ν (Nakamoto 1978; Colthup et al. 1975)

$$\nu = \frac{1}{2\pi} \sqrt{k \left(\frac{1}{m_1} + \frac{1}{m_2} \right)} \quad (32)$$

where k is the force constant and ν is the frequency of vibration.

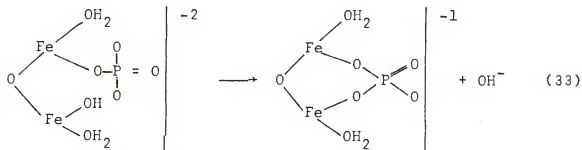
The experimental observations of frequency of vibration of a crystal are due to bond vibrations of atoms within the unit cell. Such vibration may help us to determine the nature of the atoms composing the unit cell by comparison to known polyatomic vibrations. Because of the interactions, the symmetry of a molecule is generally lower in the crystal-line state than in the isolated state. The isolated PO_4^{3-} ion is of tetrahedral form (Nakamoto 1978):



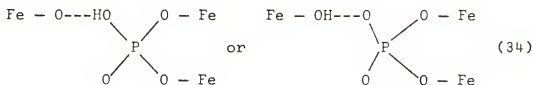
The above tetrahedral structures predict two infrared active fundamentals, one is stretching (ν_3) and the other (ν_4) is bending.

Infrared Identification of the Forms of P Adsorption

From their studies, Hingston et al. (1974) proposed the reaction



Parfitt et al. (1975) identified a form of phosphorus which can be considered to be completely within the goethite structure, since the phosphate is bound with two Fe atoms and is H-bonded to a third Fe.



Such a chemical binding of phosphate on the goethite surface is said to be specifically adsorbed, and can be considered as the formation of a new solid phase or growth of the solid phase.

Colloid or Soil Surface Effects

Substances dissolved in soil solution can move by molecular or ionic diffusion resulting from a concentration

gradient within the solution, or by mass flow of the soil solution. This is complemented by sorption of the ions onto the soil surface, or by a combination of these factors. The above phenomena occur simultaneously and are described by the following equation of de Camargo et al. (1979):

$$\frac{da}{dt} = A \frac{d^2a}{dx^2} - B \frac{da}{dx} - C \frac{db}{dt} - D \frac{d\Psi}{dx} \quad (35)$$

where a is the ion concentration in the soil solution, b is the amount of the ion adsorbed, x is the distance of the ion from the electric potential effect due to the surface charge on the charged solute. In Eq. (35), the constants are A which is a coefficient combining diffusion and hydrodynamic dispersion (cm^2/hour), B is the average pore density derived from the volumetric water content and C is the average pore water velocity, and D is the ratio between soil bulk density and volumetric water content.

In a soil system where the terms Bda/dx and $Dd\Psi/dx$ approach zero in a soil column of a semi-infinite length, over a small time t , Eq. (35) can have the following solution given by Lingstrom et al. (1968):

$$a(x,t) = a_0 \operatorname{erfc} \left[\frac{x}{2\sqrt{Kt}} \right] \quad (36)$$

where a_0 is the initial concentration, and K is a constant depending on the free energy of adsorption.

Root Effects

The effect of roots in a soil solution arises because ions movements occur into and out of the roots, with the net balance being an influx. This uptake is mainly associated with ion transport by diffusion and mass flow and is proportional to the concentration at the root surface. It is assumed that the rate of plant uptake is equal to the rate of loss of the solute, so that the reaction is:

$$\frac{da}{dt} = -\beta a \quad (37)$$

where t is the reaction time, and β is a constant. A solution of the above differential equation is given by Baldwin et al. (1973) in the following form:

$$a = a_0 \exp \left[-wt / \left(w_1 + \frac{w_2 x^2}{x^2 - r^2} \ln \frac{x}{r} \right) \right] \quad (38)$$

where a_0 is the initial concentration in solution, and where w , w_1 , and w_2 are constants, r is the root radius, and x is the distance from the root surface. This equation describes the change of the solution concentration at a certain distance from the root surface with time.

CHAPTER II KINETICS OF ADSORPTION AND DESORPTION

The interfacial region between soil colloid and solution is a center of intensive chemical and physical activities. The type of activities retaining our attention here is the adsorption and desorption processes of ions.

Adsorption

The adsorption of an ion on the colloid surface can be considered as a second order reaction involving an ion (A) and the sites (S) on the surface:



where k_1 is the rate constant of adsorption.

By assuming that the reacting sites on the colloid surface are reacting species equivalent to (A), then

$$-\frac{dA}{dt} = k_1[A]^2 \quad (40a)$$

and rearranging this is

$$\frac{dA}{[A]^2} = -k_1 dt \quad (40b)$$

or can be written as

$$\frac{1}{[A]} - \frac{1}{[A]_0} = k_1 t \quad (41)$$

The plot of $1/[A]$ versus time t should yield a straight line.

Desorption

The desorption of any adsorbed ion (AS) can be considered as a pseudo-first order reaction:



where k_2 is the rate constant of desorption. By differentiation of Eq. (42), the following can be obtained:

$$\frac{d[A]}{dt} = k_2[AS] \quad (43)$$

And by integrating the above differential equation, this becomes

$$[A] = [A]_0 \exp(k_2 t) \quad (44)$$

where $[A]_0$ is the initial concentration of the ion specie A, t is the reaction time, and k_2 is the rate constant of desorption.

Adsorption and Desorption Relationships

Since the adsorption and desorption phenomena are simultaneous a combination of the Eq. (41) and Eq. (44) is formed as follows:

$$A + S \xrightleftharpoons[k_2]{k_1} AS \quad (45)$$

$$d[A]/dt = -k_1[A]^2 \quad (46)$$

$$d[AS]/dt = k_2[AS] \quad (47)$$

where A, S, t, k_1 , and k_2 are described in the precedent

sections. By dividing the Eq. (46) and Eq. (47), and rearranging, it can be obtained:

$$\frac{d[A]}{d[A]^2} = \frac{k_1}{k_2} \frac{d[A]}{[A]}$$

$$1/[A] - 1/[A]_0 = (k_1/k_2) \ln([AS]/[AS]_0) \quad (48)$$

If we set $a = 1/[A] - 1/[A]_0$ and $b = [AS]$, then Eq. (48) can be written as

$$b = b_0 \exp\left(\frac{k_2}{k_1} a\right) \quad (49)$$

where b_0 is the amount initially adsorbed.

The above equations combining adsorption and desorption phenomena are valid only at equilibrium, there is need to propose another model combining adsorption and desorption but valid at any reaction time.

A Kinetic Model for Adsorption-Desorption

Energy Constant Characteristic of the Phase

For a collision to be effective in producing molecular species from reactants, some amount of energy must be available to allow for the necessary bonds to break and be formed. In 1889, Arrhenius suggested that molecules must get into an activated state before they become reactive. In any system, an equilibrium exists between ordinary and active molecules and only the latter are rich enough energetically to undergo reaction

$$A \rightleftharpoons (A-B)^{\#} \rightleftharpoons B \quad (50)$$

where $(A-B)^{\#}$ is the spatial configuration of the transition state. The species $(A-B)^{\#}$ does not represent the active molecule of Arrhenius. His active or energized species are rather a few reactant molecules having sufficient energy to get into the transition state, $(A-B)^{\#}$, or activated complex condition, but not necessarily having the spatial configuration corresponding to the transition state (Eying and Eying 1963).

Let us consider the following system

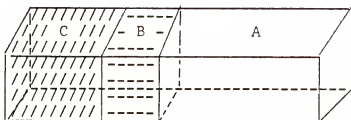


Figure 1. Schematic representation of solid-interface-solution system.

where A is the solution phase, B is the interfacial phase, and C is the solid phase. Here A, B, and C are different degrees of energized species of the same ion (or molecule) with respect to the solid surface; these are considered characteristic of solution, interfacial, and solid phase, respectively. The surface sites at which ions take the

form C are at random on the solid surface. It is believed that the sites associated with the lowest energy are the first to be filled by the ions taking the form C.

Formulation of the Model

In the system described above, it can be assumed that the following type of reaction is taking place:



where A, B, and C are as described previously and subscripts a, b, and c designate the amounts of the ion in the forms A, B, and C per unit volume of the system. The terms k_1 k_2 are the rate constants for forward reaction and reverse reactions, correspondingly are k_{-1} and k_{-2} .

The rate of a reaction can be expressed by the rate of change of the concentration of the ion species:

$$\frac{da}{dt} = k_{-1}b - k_1a \quad (52a)$$

which in expanded form becomes

$$\frac{db}{dt} = k_1a - k_{-1}b + k_{-2}c - k_2b = k_1a - (k_{-1} + k_2)b + k_{-2}c \quad (52b)$$

and

$$\frac{dc}{dt} = k_2b - k_{-2}c \quad (52c)$$

Since any colloid cannot, within a finite period of time, indefinitely fix an ion in the C energy form, then c must reach a maximum at equilibrium. In Eq. (52b), it is assumed that k_{-2} is very low compared to k_2 .

The simultaneous solution of the differential for Eq. (52a) and Eq. (52b) is

$$a = \alpha e^{w_1 t} \quad \text{and} \quad b = \beta e^{w_2 t} \quad (53)$$

where

$$\alpha w_1 e^{w_1 t} = -k_1 \alpha e^{w_1 t} + k_{-1} \beta e^{w_1 t} \quad (54a)$$

and

$$\alpha w_2 e^{w_2 t} = k_1 \alpha e^{w_2 t} - (k_{-1} + K_2) \beta e^{w_2 t} \quad (54b)$$

From the Eq. (54a) and Eq. (54b), the coefficients α and β can be determined as a function of the rate constants.

In any soil-solution system, equilibrium is attained when the rate of change of each ion in the different phase becomes nil, so that it is then

$$\frac{da}{dt} = 0 \quad \frac{db}{dt} = 0 \quad \frac{dc}{dt} = 0$$

such that $k_2 b - k_{-2} c = 0$ and $c=s$, then the term β is deduced as

$$\beta = s \frac{k_{-2}}{k_2} e^{-w_2 t_0} \quad (55)$$

Similarly, if $k_{-1} b - k_1 a = 0$, then substituting in the β value, α is found to be

$$\alpha = s \frac{k_{-1}}{k_1} \frac{k_{-2}}{k_2} e^{-w_1 t_0} \quad (56)$$

In the initial a and b expressions, shown in Eq. (53), it can be shown that

$$a = s \frac{k_{-1}}{k_1} \frac{k_{-2}}{k_2} e^{w_1(t-t_o)} \quad (57a)$$

and

$$b = s \frac{k_{-2}}{k_2} e^{w_2(t-t_o)} \quad (57b)$$

The Eq. (52c) can be expressed in the following as a first order linear differential equation:

$$\frac{dc}{dt} + k_{-2}c = \beta k_2 e^{w_2 t} \quad (58)$$

The solution to this differential equation to satisfy the condition where $c = 0$ at $t = 0$ can be written in the form

$$c = \frac{\beta k_2}{k_2 + w_2} \left[e^{w_2 t} - e^{k_{-2} t} \right] \quad (59a)$$

If we assume that k_{-2} is negligible, c can be further simplified

$$c = \frac{\beta k_2}{k_2 + w_2} e^{w_2 t} \quad (59b)$$

where w_1 and w_2 are constants.

CHAPTER III THERMODYNAMICS OF ADSORPTION-DESORPTION REACTION

At the microregion in the colloid or soil solution extending from the surface to the outer limit of the first adsorbed layer, it is assumed that the electrical effect due to surface charge is negligible to avoid the difficulty in estimation of the electric field effect. In this microregion, there is ion interaction between both the surface and the electric potential effects (which are induced by the surface charge).

The Surface Charge

The colloidal behavior depends on how the surface charge originated. There are two type of colloidal charges. The first type has the charges due to crystalline imperfection, such as isomorphic substitution of Si^{4+} by Al^{3+} or by other cations such as (Mg^{2+}) having a lower charge. This type of charge is found in the crystal lattice of clays such as montmorillonite and vermiculite. In these cases, the charge density is constant per unit of surface area. The second type occurs where the surface charge may be created by preferential adsorption of a certain ion, such as that by hydroxyl or phosphate ions. In this case, the charge arises at the exterior edge of crystals or lattice, thereby inducing a constant surface potential (van Olphen 1977; Bolt 1976).

Gouy-Chapman and Stern Theories of the Double-Layer

From Gouy-Chapman theory, the charge density can be deduced considering the electroneutrality condition (van Olphen 1977; Sennet and Olivier 1965):

$$\sigma = -\int_0^{\infty} \rho dx \quad (60)$$

$$\sigma = \frac{\epsilon a k T}{2\pi} \left[\exp(z_i e \Psi_0 / 2kT) - \exp(-z_i e \Psi_0 / 2kT) \right] \quad (61)$$

where ρ is the space charge density (or net sum of positive and negative ion concentration, σ is the surface charge, and Ψ_0 is the surface potential. The Gouy-Chapman theory gives an over-estimation of the double layer capacity, namely

$$K = (8z^2 e^2 a / \epsilon k T)^{1/2} \quad (62)$$

where K is the reciprocal of the double layer thickness, a is the ion concentration, e is the electron charge, z is the valence of the ion, and ϵ is the dielectric constant.

Stern recognized the importance of the ion sizes near the surface. He proposed that the counter ions could be divided between a diffuse layer and an immobile surface layer of thickness δ able to contain a maximum number of counter ions per unit of surface area. This may be expressed as

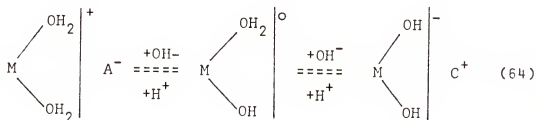
$$\sigma = \frac{n \sigma_m}{n + A \exp(-ze \Psi \delta / kT + \phi)} + \sqrt{\frac{\epsilon a k T}{2\pi}} \exp(ze \Psi \delta / 2kT) - \exp(-ze \Psi \delta) \quad (63)$$

where σ_m is the charge corresponding to a monolayer of

counterions, ϕ is the van der Wall energy, A is the frequency factor, $\Psi\delta$ is the electric potential at the Stern Layer.

Zero Point of Charge (ZPC)

On a metal oxide surface, charges are created by the adsorption and desorption of H^+ or OH^- ions which are affected by their concentrations in solution. The Parks and de Bruyn (1962) model is



where M is Al or Fe with A^- and C^+ are the associate anion and cation, respectively. From the Eq. (64), it can be seen that there is a pH at which the net surface charge is zero; this point is termed the zero point of charge (ZPC).

For metal oxides, such as described above, H^+ and OH^- ions are potential determining ions. By approximation to the Nernst equation, Keng and Uehara (1974) reported that

$$\sigma_o = \frac{RT}{F} \ln \frac{H^+}{H_o^+} \quad (65)$$

where R is the gas constant, T is the absolute temperature, F is the Faraday constant, and $\Psi_o \ll 25$ mV; the Gouy-Chapman double layer equation is reduced according to

$$\sigma_o = \frac{K\epsilon}{2\pi} \psi_o = \frac{K\epsilon}{2\pi} (0.059)(pH_o - pH) \quad (66)$$

Thermodynamics of Adsorption

Effect of the Electric Field

In this system introduced in Fig. (1), the compartments A, B, and C can be considered as being three phases of a particular ion at different potential energy levels. In each phase, molecules are at different energy levels and varying within a range of potential characteristics of each phase.

Around a colloid center, the ions exhibit a Boltzman type distribution:

$$c = b \exp [-F(\psi_c - \psi_b)/RT] \quad (67a)$$

$$b = a \exp [-F(\psi_b - \psi_a)/RT] \quad (67b)$$

Supposing that $\psi_a = 0$, it can be shown that

$$\psi_o = \psi_c = -\frac{RT}{F} \ln \frac{c}{a} \quad (67c)$$

where ψ_o is the surface potential, ψ_b and ψ_a are electric potentials that is characteristic of the phases B and A, respectively.

Free Energy as a Function of Distance

From the outer limit of the Stern layer, both Gaussian and Gouy-Chapman concepts can be applied to a particular ion. The movement of an ion (or molecule) results from a succession of collisions that may move it at random in a

positive or negative direction. These ionic concentrations follow the Gaussian distribution:

$$a = \frac{M}{2(\pi Dt)^{1/2}} \exp(-x^2/4Dt) \quad (68)$$

where M is the amount of substance deposited at the plane when $x = 0$ at the time $t = 0$, and D is a constant. Assuming that the Gouy-Chapman distribution holds in the following equation:

$$\Psi = \Psi_0 \exp(-Kx) \quad (69)$$

where the free energy can be expressed as

$$G_{i,m} = G^0 + zF\Psi + RT \ln a \quad (70a)$$

and

$$G_{i,m} = G^0 + zF\Psi_0 \exp(-Kx) + RT \ln \frac{M}{2(Dt)^{1/2}} - \frac{RTx^2}{4Dt} \quad (70b)$$

At constant time t, this expression becomes

$$\frac{dG}{dx} = -zF\Psi_0 K e^{-Kx} - \frac{RT}{2Dt} x \quad (71)$$

The limit between the physically adsorbed layer and the completely free ion in the phase A may be defined when $dG/dx=0$. If we set $y = -Kx$ and $\gamma = -RT/2Dt/zF\Psi_0 K$, then the expression can be written

$$e^y - \frac{\gamma}{K} y = 0 \quad (72)$$

and become

$$y^2 + 2y(1 - \frac{1}{K}) + 1 = 0$$

where

$$(e^y = 1 + y + 1/2 y^2 + \dots)$$

When this quadratic equation gives two roots, they may be indicators of the transition states between different degrees of adsorption.

Free Energy for Irreversible Fixation

The active transport of an ionic substance against the gradient potential is determined by the difference between the total potential within each phase (A, B, and C). The maximum energy, other than expansion work for a change of ion activities, is expressed by $G_{i,m}$ at constant temperature and pressure. The transfer of ions between the phase B and C is due to a potential energy minimum for phase C written as $G_{i,m}^C$ and maximum for phase B written as $G_{i,m}^B$. In this case

$$G_{i,m}^C = z_i F \psi^C + X_i \quad (73)$$

and, correspondingly,

$$G_{i,m}^B = z_i F \psi^B + RT \ln b \quad (74)$$

where $G_{i,m}$ is also the Gibbs free energy of the ion i per unit mole, X_i is defined as the minimum energy for irreversible fixation (including only the electro-chemical energy), F is the Faraday constant, ψ^B and ψ^C are the electric potential in the phases B and C, and the term $RT \ln b$ is the chemical potential. The transfer of ions between the phases B and C is governed by the difference in total energy between the two phases,

$$\Delta G_{i,m} = -4\delta\sigma z_i F + RT \ln s^{\frac{k-2}{k_2}} + RTw_2(t - t_0) - X_i \quad (75)$$

where $\Psi = \Psi^C - \Psi^B = \Psi^O - \Psi^\delta = 4\pi\delta\sigma$ which is the Gaussian equation for a molecular condensor. This by substitution gives

$$\Delta G_{i,m} = 4\pi\delta\sigma z_i F + RT \ln s^{\frac{k-2}{k_2}} - X_i \quad (76)$$

When the conditions are at equilibrium, or $\Delta G = 0$ and $t = t_0$, then

$$X_i = -4\pi\delta\sigma z_i F + FT \ln s^{\frac{k-2}{k_2}} \quad (77)$$

It is assumed that the minimum energy X_i is independent of the state of equilibrium, then for a given colloid surface which has a particular surface charge, the free energy change $\Delta G_{i,m}$ is reduced to

$$\Delta G_{i,m} = RTw_2(t - t_0) \quad (78)$$

Relationship of Surface Charge to Surface Potential

During the overall transfer of ions from the phase A to phase C at equilibrium conditions, after substituting the X_i value of Eq. (77) and assuming $\Psi^A = 0$, the relationship becomes

$$d\Psi_0 = \frac{4\pi\delta}{a_i F} d\sigma \quad (79)$$

where δ is the Stern layer thickness, σ is the surface charge, F is the Faraday constant, and a_i is the ion valence.

Surface Tension and Specific Adsorption

In the interfacial colloid-liquid region, some ions may enter into the coordination shell of surface atoms. As a result, there is a modification of the colloid surface (A) (expansion or contraction). This work required to expand or contract the surface when divided by the change in surface area is the surface tension (γ) (Atkins 1978). The following series demonstrates the relationship:

$$G_i^C = z_i F \Psi^C + A \gamma \quad (80a)$$

$$G_i^C = z_i F \Psi^C + X_i^C \quad (80b)$$

Differentiating the Eq. (80a) and Eq. (80b) gives

$$dG_i^C = z_i F \Psi^C dc + z_i F cd \Psi + \gamma dA + A d\gamma \quad (81a)$$

$$dG_i^C = z_i F \Psi^C dc + z_i F cd \Psi + X_i^C dc + c dX_i^C \quad (81b)$$

However, it is known that

$$dG_i^C = z_i F \Psi^C dc + X_i^C dc \quad (82a)$$

$$dG_i^C = z_i F \Psi^C dc + \gamma dA \quad (82b)$$

By comparing Eq. (81a) to Eq. (82b) and Eq. (81b) to Eq. (82a) it follows that

$$c dX_i^C = A d\gamma \quad (83)$$

The differentiation of Eq. (77) gives $dX_i^C = -4\pi\delta z_i F \cdot d\sigma$, so it can be deduced that

$$\frac{d\gamma}{d\sigma} = \frac{-4\pi\delta z_i}{A} c \quad (84)$$

CHAPTER IV MATERIALS AND METHODS

Goethite Preparation

Three goethite preparations were made by mixing separately an equal volume (50 ml) of 1 N $\text{Fe}(\text{Cl})_3$ with a similar volume of 2 N NaOH, 1 N NaOH, or 0.5 N NaOH in order to have OH/Fe mole ratios of 6, 3, and 1.5, respectively, in the mixtures. The suspensions were allowed to age for one week to induce crystal formation and growth. The addition of phosphorus to the goethite preparation was made for $\text{P/Fe} = 3.2$ ratio both at the beginning and by adjustment at the end of ageing process (one day of phosphorus reaction is allowed). In order to examine the effects of phosphorus concentrations on goethite crystallization, different levels of phosphorus in 2 N NaOH were mixed with 1 N $\text{Fe}(\text{Cl})_3$ and allowed to age. After one week of ageing the suspension at either room temperature or at 55°C , the samples were washed by dialysis against distilled water during one week; the water was changed after intervals not greater than 12 hours. At the end of the ageing process and washing, the samples were freeze-dried.

The existence of hydroxyl deformational vibrations in the region 1200 to 1000 cm^{-1} was investigated by two methods:

1) goethite and phosphated goethite were digested in D_2O for 24 hours to replace the surface OH by OD, or 2) phosphated goethite samples were equilibrated with different salts (0.1 N KCl , 0.1 N KNO_3 , and $0.1 \text{ N Na}_2\text{SO}_4$) and water to displace surface phosphates. The samples were separated from solution and dried for the infrared spectroscopy studies.

An attempt was made to prepare $FeOOD$ by digesting three times 0.9 g of $FeCl_e \cdot 6H_2O$ in D_2O and drying the suspension in order to make $FeCl_3 \cdot 6D_2O$. The residues were dissolved in 10 ml of D_2O and mixed with 10 ml 2 N NaOD ; the suspensions were then aged and dried as described above.

Infrared and X-Ray Diffraction Techniques

One milligram of the freeze-dried sample was mixed with 400 mg KBr to make pellets samples used for the infrared study. The infrared spectra are obtained by using Perkin-Elmer 567 grating infrared spectrophotometer.

Prior to X-ray diffraction analysis using a general electric XRD700 instrument, and thin films of goethite samples were made on glass slides and allowed to air dry.

Some Factors Affecting the Kinetics of Adsorption-Desorption

The adsorption or desorption isotherm is obtained by plotting the amount of ion adsorbed or desorbed per unit weight of adsorbent versus the solution concentration. The

solid and the solution were equilibrated through agitation for selected periods of time and temperatures. The equilibrium solution was removed after centrifugation and the phosphorus concentration determined through blue color development as ascorbic acid molybdophosphoric complex.

Effects of pH

The adsorption for different periods of times (0 to 72 hours) was done by equilibrating goethite or soils with phosphorus solution (5 μ g P/ml) or (20 μ g P/ml) adjusted to pH 2, 4, 8, 9.5, and 11. Solid phase was separated by centrifuging at 5000 revolutions per minute (rpm). Phosphate desorption was carried out on samples which reached the equilibrium state. The desorption was conducted in water, adjusted to the above pH, during 20 minutes, 6 and 12 hours. The pH of the solution was measured by placing the glass electrode in the supernatant after centrifugation.

Effects of the Supporting Electrolytes

The effects of the type of cations on the adsorption were studied by mixing 20 mg of goethite with 20 ml each of the phosphate solutions containing 1, 3, 5, and 10 μ g P/ml in 0.01 M salts of NaCl, CaCl₂, and AlCl₃, each in separate experiments. With soils, the phosphate solution concentrations used were 0, 10, 20, 40, and 80 μ g P/ml. The extent that each of the cations (Ca, Na, and Al) contributed to the

degree of reversibility of the adsorbed phosphate was studied by conducting the desorption with solution of the corresponding electrolyte (as in the adsorption) but without phosphate. A comparison of the phosphate desorption by different anions in various salts (KCl , K_2SO_4 , KNO_3 , KClO_4 , and NaOH) was made for goethite-P solution (one gram of solid with one liter of salt solution where the goethite had previously been treated with $5 \mu\text{g P/ml}$).

Time Effects on Adsorption and Desorption

Adsorption of phosphates on goethite-solution containing 0, 1, 3, 5, 7, and $10 \mu\text{g P/ml}$, and on soil-solution containing 0, 5, 10, 20, 40, and $80 \mu\text{g P/ml}$ was investigated after equilibration during different periods of time ranging from 1/10 hour to 80 hours. At the end of each reaction time, the solid-solution was centrifuged and the phosphate concentration remaining in the supernatant solution determined. The solid/solution ratio was 1/1000 for goethite-solution and 1/20 for soil-solution. Kinetic studies of phosphate adsorption were done at different conditions: 1) when different types of electrolytes were used, 2) for one electrolyte (CaCl_2) at different concentrations ($.01 \text{ N Ca}$, 0.1 N Ca , 1.0 N Ca), and 3) at pH 2 and pH 10. After the adsorption proceeded until the equilibrium state was reached, desorption was conducted during 20 minutes, 6 and 12 hours in order to determine the minimum time required for complete

desorption of this form of phosphate. This minimum time was also employed during desorption of phosphate when using either a desorbing solution at selected pH (2 to 11) or for different electrolytes. For those soils where it was observed that phosphate sorption did not follow the Langmuir isotherm, an attempt was made to determine the extent of changes in aluminum and iron phosphate by using the method of Peterson and Corey (1966). For aluminum phosphate, one gram of soil sample was washed with 2 N NaCl to remove exchangeable cations, the suspension was centrifuged and the supernatant solution discarded. Then 20 ml of 0.5 N NH_4F at pH 8.2 were added and the suspension was shaken for an hour and then centrifuged for the P determination. For the iron phosphate fraction, the samples were washed with 2 N NaOH solution, centrifuged, and the supernatant retained for P determination.

Surface Charge as Affected by Phosphate Adsorption

The method of Lavardiére and Weaver (1977) was used to determine the net electric charge. The procedure was to add 20 ml each of 0.01 N CaCl_2 and 1.0 N CaCl_2 solutions per one gram of soil sample or 20 mg of goethite. Subsequent titrations of the suspensions were made with 0.01 N HCl or 0.01 N NaOH, by adding 0.1 to 0.3 ml at a time from a microburet at 2-minute intervals. Continuous stirring was maintained and the pH read before the addition of either base or acid.

A blank titration was made for the same volume of CaCl_2 solution. The amount of H^+ or OH^- adsorbed at a given pH was calculated by the difference between the amount of H^+ or OH^- added and that required to bring the blank solution of the same volume and salt concentration to the same pH as the soil or goethite.

Soil pH, Iron Oxide, and Extractable P

The soils used were obtained from Georgia (Cecil, Ap horizon), Colorado (roadside cut near Ft. Collins), and Kenya (latosol, sampled at 15-30 cm, near Kabete).

The pH was measured in 1:1 soil to solution suspension for 10 g of soil with 10 ml of H_2O or 10 ml of 1 N HCl, using a glass electrode. Iron oxide was determined by the dithionite-bicarbonate extraction and colorimetric determination of Fe as the ferrous orthophenanthroline complex. Extractable P was determined by three of the methods outlined by Ballard (1979). These data are shown in Table 1.

Table 1. Soil pH, iron oxide and extractable P.

Soils	Georgia	Colorado	Kenya
pH(H ₂ O)	5.88	8.17	6.20
pH(KCl)	4.95	7.44	5.75
% Fe ₂ O ₃	2.24	0.67	3.95
P, ppm	0.05 <u>N</u> HCl + 0.025 <u>N</u> H ₂ SO ₄ [*]		
	5.60	0.30	0.40
P, ppm	0.03 <u>N</u> NH ₄ F + 0.1 <u>N</u> HCl [*]		
	13.00	7.40	1.40
P, ppm	0.5 <u>M</u> NaHCO ₃ [*]		
	2.80	1.20	1.60

*Reagents described by Ballard (1974)

CHAPTER V RESULTS AND DISCUSSION

Goethite and Phosphated Goethite Studies by InfraRed Spectroscopy

After the mixing of FeCl_3 and NaOH solutions, some precipitates formed, but the particles formed at precipitation were not yet crystalline. The changes in precipitates to crystals originated from a discrete center or crystal nuclei (twinned and acicular crystals) produced by different mechanisms (Atkinson et al. 1968). The conditions governing the formation and nature of these crystal nuclei are not well known. Apparently, the number of crystal nuclei was increased by both temperature and hydroxyl ion concentrations. Iron and hydroxyl ions would be attracted to the centers of crystal growth as they lose their energies. As iron and hydroxyl ions were involved in the formation of the crystal, ageing reactions follow the sequence of lepidocrocite to goethite (Murphy et al. 1975). Another way would be that ferrhydrite forms first or just goethite was formed. The growth of the crystal occurred as the ions change phase during deposition from the solution. Hsu (1972) found that the removal of hydroxyl ions from the solution resulted in a drop in pH value of the solution as the time increased.

Since the ions are changing phase from the solution (higher degree of randomness) to the solid phase (lower degree of randomness), the entropy change during the process from solution to crystalline phase must be negative. The entropy of ions within the crystal would be lower than those at the crystal surface. From infrared spectra, Kiselev and Lygin (1975) believed it was possible to estimate from adsorption entropy what was the degree of freedom of the adsorbed molecules.

Goethite Structure Identification by Infrared

The 4000 - 2000 cm^{-1} Region

The goethite structure was interpreted through the identification of OH and FeO vibrations. The hydroxyl ion vibrations occurred at two strong bands in the 3700 - 2000 cm^{-1} region, centered at 3400 cm^{-1} and 3200 cm^{-1} (see Fig. 2 and Fig. 3). According to Nakamoto (1978), lattice water absorbed at 3550 - 3200 cm^{-1} , he reported that the strong band centered at 3400 cm^{-1} was due to anti-symmetric and symmetric OH-stretching of water. It could easily be recognized that the 3400 cm^{-1} band was not characteristic of goethite crystal structure since this band appears even when no goethite is present, as determined by X-ray diffraction which showed no crystalline material. It is of interest to observe that the intensity of the 3200 cm^{-1}



Fig. 2. Infrared bands of (A) goethite; (B) phosphate added to goethite at the end of ageing; and (C) phosphate added to goethite at the beginning of ageing. Curves A, B and C are for 22° C and curves A', B', and C' are for 55° C.

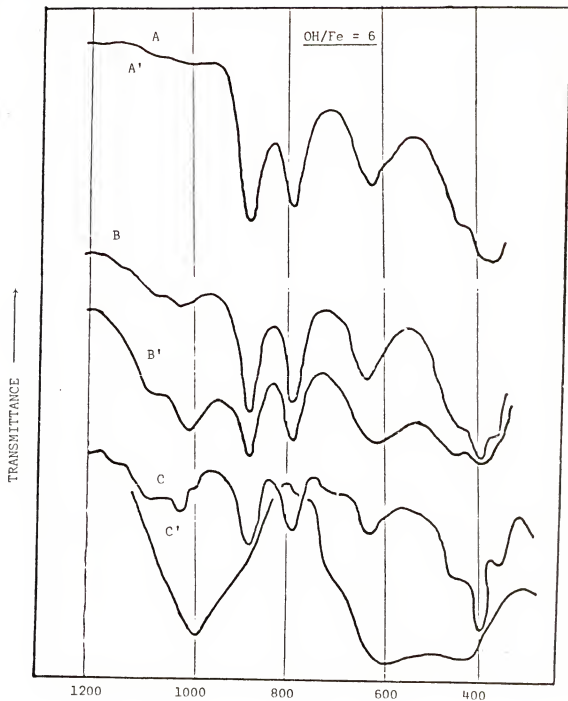
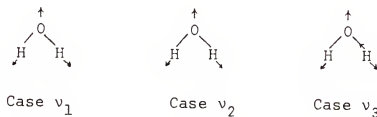


Fig. 3. Infrared bands of (A) goethite; (B) phosphate added to goethite at end of ageing; (C) phosphate added to goethite at beginning ageing. Curves A, B, and C are for 22° C, and curves A', B', and C' are for 55°C.

band decreased as the OH/Fe ratio in the ageing solution decreased. The band centered at 3200 cm^{-1} appeared only if goethite structure was present. As a result, it was concluded that the 3200 cm^{-1} band corresponded to structural Fe - OH stretching.

The $2000 - 3000\text{ cm}^{-1}$ Region

After goethite was freeze-dried, not all the adsorbed water was removed. Nakamoto (1978) indicated that the relative velocity of the oxygen nucleus compared to that of hydrogen nucleus is small. This meant that the surface binding of water through the oxygen atom to goethite would not induce a significant change in the overall water vibration which could be observed at around 1620 cm^{-1} as depicted for water structure below



The above three normal modes of vibration in H_2O are infrared active. The bending vibration v_2 is centered at 1620 cm^{-1} and the water stretching bands (v_1 and v_3) vibrate in the 3400 cm^{-1} region.

The 1300 - 700 cm^{-1} Region

The two main bands at 890 and 790 cm^{-1} would be assigned to Fe-OH bending vibration of the structural hydroxyls. Busca et al. (1978) supported this finding by observing that the structural OH in $\alpha\text{-FeOOH}$ disappeared upon heating to form $\alpha\text{-Fe}_2\text{O}_3$. The appearance of the 890 and 790 cm^{-1} bands always indicated goethite crystallization, which can be observed in Fig. 3, 4, 5, 6, 7, 9, 10 and 11. From the above mentioned figures, it was observed that for each OH/Fe ratio, the way in which phosphate was added had an effect on the degree of goethite crystallization. From Fig. 5, as reported by Farmer and Palmieri (1975), typical goethite could be identified by the Fe - OH bending vibration at 890 cm^{-1} and 790 cm^{-1} . In Fig. 3, where OH/Fe = 6, there are also strong bands at 890 and 790 cm^{-1} in all cases, except when phosphate is added at the beginning of ageing of the suspension at 55°C. In the latter case, the increase of temperature to 55°C favored preferential phosphate binding to the iron which was observed by the strong vibration at 1000 cm^{-1} . As shown in Fig. 3c, phosphate was within the goethite structure because there was both the P - O(Fe) vibration at 1000 cm^{-1} and the surface binuclear $(\text{FeO})_2\text{POOH}$ vibrations at 1190, 1100, and 1030 cm^{-1} . When OH/Fe = 3, it was not possible to have phosphate within the crystal because there was no crystallization at room temperature. However

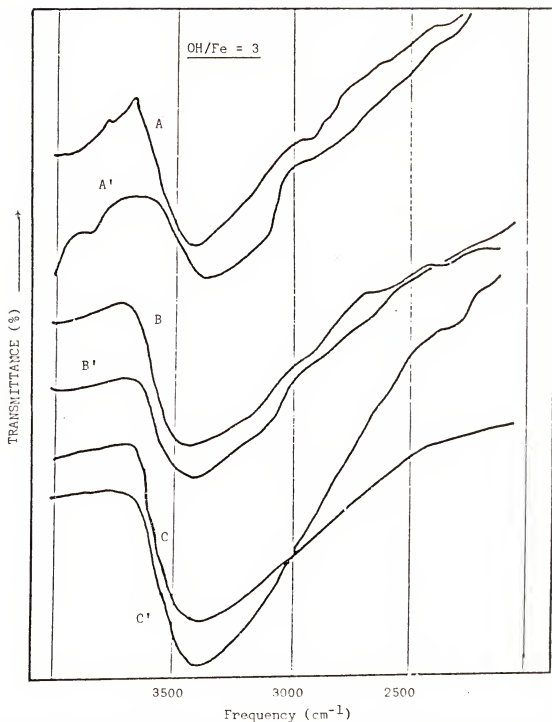


Fig. 4. Infrared bands of (A) goethite; (B) phosphate added to goethite at end ageing; and (C) phosphate added to goethite at beginning ageing. Curves A, B, and C are suspensions at 22°C, and curves A', B', and C' are for suspensions at 55°C.

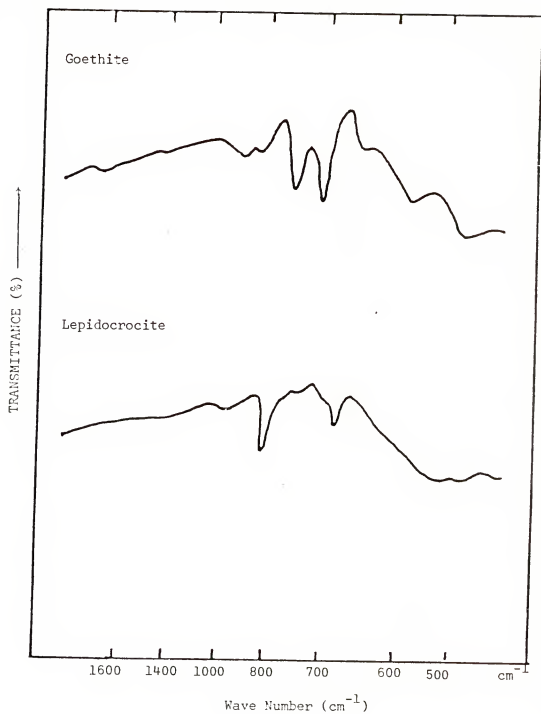


Fig. 5. After Farmer and Palmieri (1975). Infrared bands of Goethite and lepidocrocite.

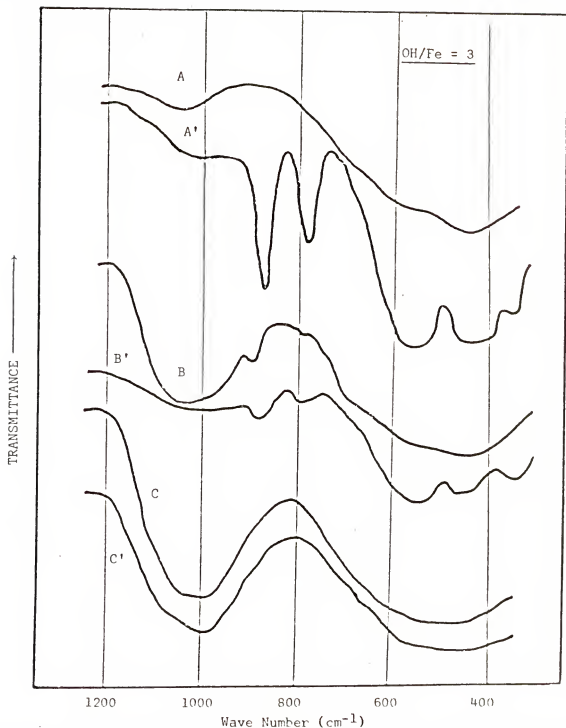


Fig. 6. Infrared bands of (A) goethite; (B) phosphate added to goethite at end ageing; and (C) phosphate added to goethite at beginning ageing. Curves A, B and C are for suspensions at 22°C and curves A', B', and C' are for 55°C.

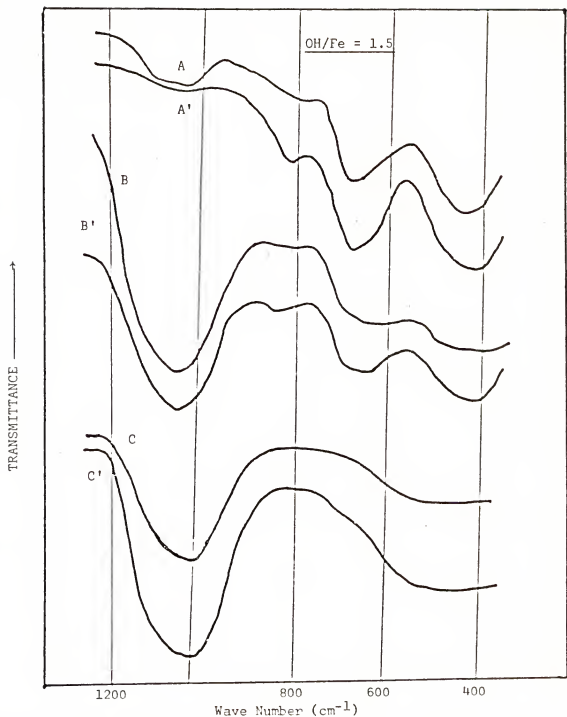


Fig. 7. Infrared bands of (A) Fe hydroxide material; (B) phosphate added to Fe hydroxide material at end of ageing; and (C) phosphate added to Fe hydroxide material at beginning of ageing. Curves A, B, C are for suspensions at 22° C and curves A', B', C' are for suspensions at 55° C.

there was weak crystallization at 55°C that favored some phosphate surface binding (see Fig. 6b). In OH/Fe = 1.5 suspension, after one week of ageing either at room temperature or at 55°C, no goethite formation was observed. There was a single, strong vibration at 1030 cm^{-1} when phosphate was added at the end of the ageing, but the vibration was at 1000 cm^{-1} when the phosphate was added at the beginning of ageing. The 1030 cm^{-1} vibration, which is the P - OH bending vibration, indicated the existence of phosphate at the surface, and the presence of the 1000 cm^{-1} vibration from the P - O(Fe) showed phosphate directly bound to iron when phosphate was added just prior to the ageing process (Parfitt et al. 1975).

Goethite Identification by X-Ray

The X-ray diffraction peaks for goethite were at 4.19 \AA , 2.70 \AA , and 2.45 \AA . In all cases, the 4.19 \AA is the most intense peak while those at the 2.70 \AA and 2.45 \AA were weak, Fig. 8. The presence of the 2.70 \AA spacing indicated that some hematite might be present. However, because the 2.45 \AA peak was present, it was believed that considerable amounts of goethite existed (Schwertman and Taylor 1977). According to their studies, it would be possible for hematite to exist along with goethite because the hydration of hematite would yield goethite with a standard free energy (ΔG°) of the reaction varying from -0.2 to 0.4 kcal/mole .

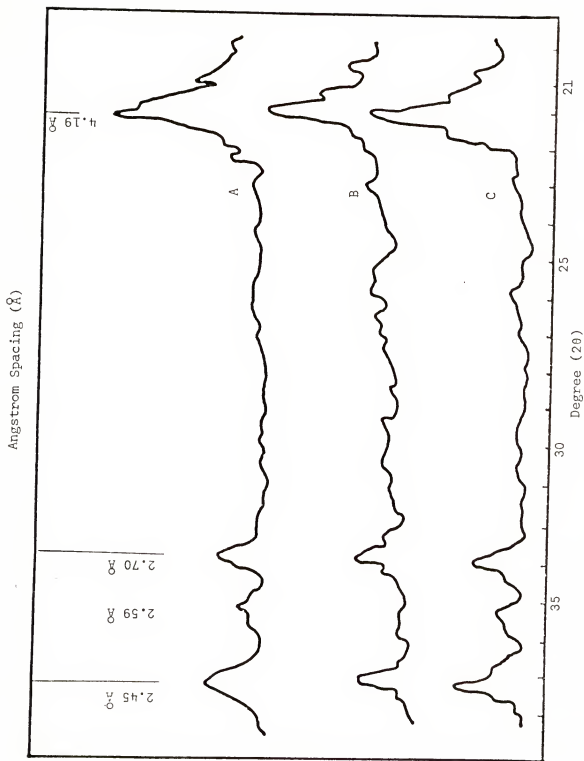


Fig. 8. X-ray diffraction patterns of (A) goethite, (B) phosphated goethite at end of ageing, and (C) phosphated goethite at beginning of ageing.

Factors Affecting Goethite Crystallization

Effect of OH/Fe Ratio

The above results indicated that the bands at 3400 cm^{-1} , 3200 cm^{-1} , 890 cm^{-1} , and 790 cm^{-1} were characteristic of the appearance of goethite. For the same ageing period, an increase in OH/Fe favored goethite crystallization. When the OH/Fe is 6, the bands at 3200 cm^{-1} , 890 cm^{-1} , and 790 cm^{-1} were strong, indicating that goethite structure was well-formed. Where OH/Fe is 3, after a week of ageing, goethite structure was apparently present only if the suspension was kept at 55°C , even then the degree of crystallization was less intense at OH/Fe = 3 than it was where OH/Fe = 6. This weak crystallization was suggested by the weak band at 3200 cm^{-1} (which took the form of a shoulder) and by the less pronounced intensities of the 890 cm^{-1} and 790 cm^{-1} bands. However, when OH/Fe is 1.5, there was no goethite crystallization even when the suspension was aged at 55°C . The above conclusion disagreed with that of Atkinson et al. (1974) who claimed made goethite was in a suspension at 28°C where OH/Fe is 2.0 when aged for 50 hours.

Phosphated goethite

The application of phosphorus weakened the goethite structure because some phosphate was probably incorporated within the lattice. In Fig. 4 and Fig. 6 where OH/Fe is 3,

the addition of phosphate to goethite suspension resulted in bands at 3200 cm^{-1} , 890 cm^{-1} and 790 cm^{-1} which were weaker than those for $\text{OH/Fe} = 6$ after ageing. When $\text{OH/Fe} = 6$ in the suspension, hydroxyl ion concentration was high enough to form the necessary bonds for the goethite structure to appear. The presence of phosphate on the goethite surface could be recognized by the appearance of bands in the $1200 - 1000\text{ cm}^{-1}$ region, but vibrational hydroxyl deformations also could occur in this same region. Parfitt (1979) stated that the $\text{P} = \text{O}$ bond had stretching vibrations in the 1190 cm^{-1} and the 1030 cm^{-1} region.

When the phosphate was added at the end of the goethite ageing, there was an appearance of $\text{P} = \text{O}$ vibration at 1190 cm^{-1} and the 1030 cm^{-1} due to $\text{P} - \text{OH}$ vibration in agreement with work by Parfitt (1979). At high temperature (55°) even when $\text{OH/Fe} = 6$, the phosphate is preferentially bonded to the iron, thereby reducing the capacity of hydroxyls ions to bind freely with iron to form goethite. As a result, there was direct binding of phosphate to iron which was confirmed by the strong band at 1000 cm^{-1} assigned to $\text{P} - \text{O}(\text{Fe})$ and by the lack of the $\text{Fe} - \text{OH}$ bending vibrations at 890 cm^{-1} and 790 cm^{-1} . This is confirmed by spectra given in Fig. 3. In Fig 9, Fig 10 and Fig 11 where suspension the OH/Fe ratio was either 6, 3, or 1.5, the increase in phosphate concentrations relative to the iron ($\text{P/Fe} = 0.032$,

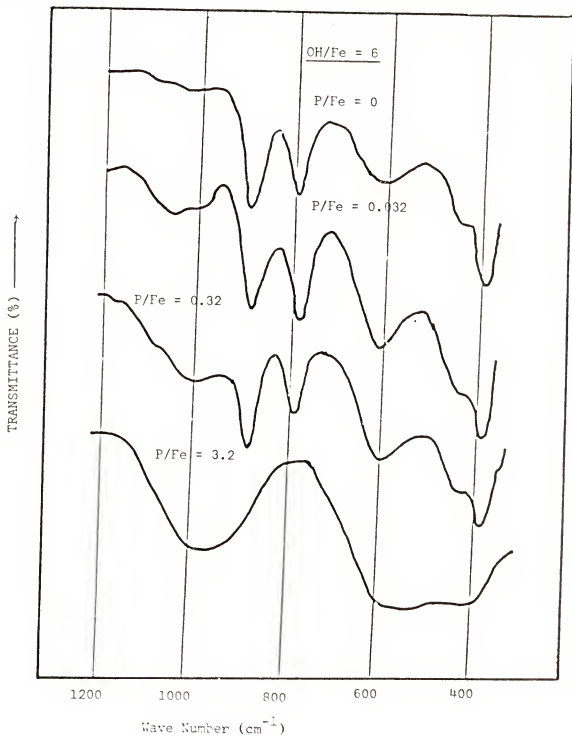


Fig. 9. Infrared bands of phosphated goethite at beginning of ageing for suspensions of various P/Fe values at OH/Fe = 6.

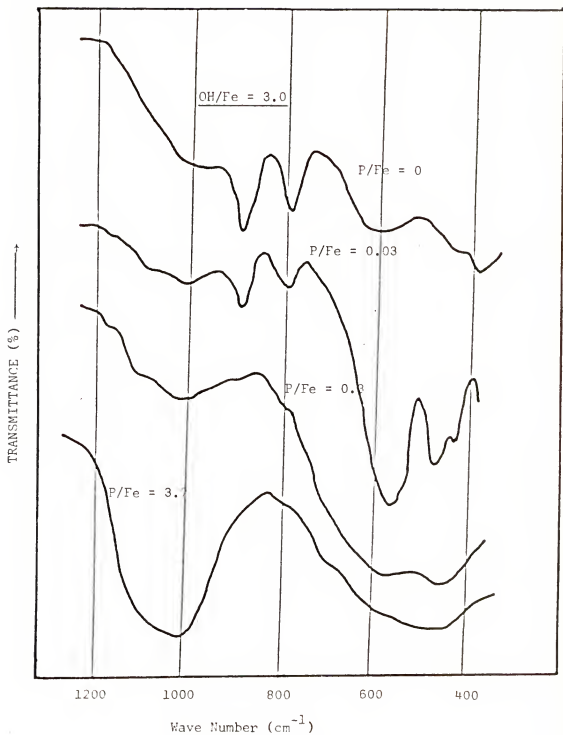


Fig. 10. Infrared bands of phosphated goethite at beginning of ageing for various P/Fe ratios at $\text{OH/Fe} = 3.0$.

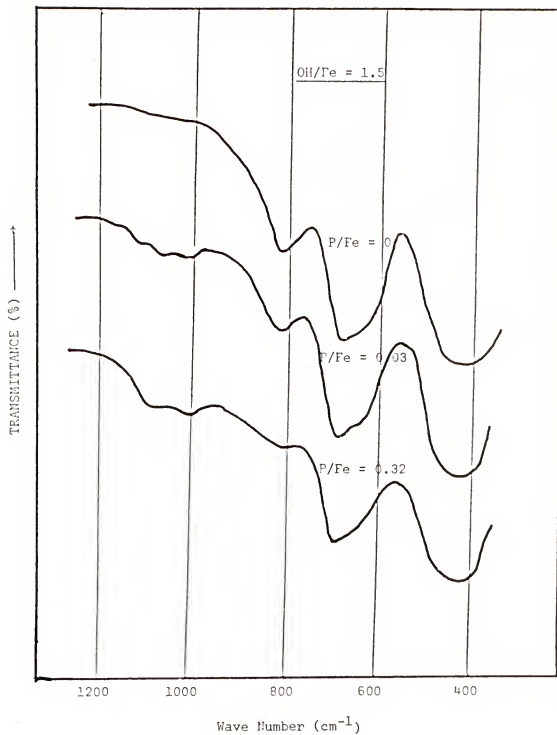


Fig. 11. Infrared bands of phosphated goethite at beginning of ageing for various P/Fe ratios at OH/Fe = 1.5.

0.32, 3.2) induced an increase in the intensity of P - O(Fe) and P - OH stretching vibration at 1000 cm^{-1} and 1030 cm^{-1} , respectively. When P/Fe was greater or equal to 0.3, these two bands overlapped, showing only one very strong band at 1000 cm^{-1} .

In order to identify the vibration of hydroxyl deformation assumed to be in the $1200 - 1000\text{ cm}^{-1}$ region, two methods were used: 1) goethite and phosphated goethite were digested in D_2O for 24 hours and 2) surface phosphate was desorbed by different anions and water. After the samples were dried, the infrared spectra were similar to those shown in Fig. 12 and Fig. 13. The weak bands due to OH deformation were displaced by OD and only the P - O(Fe) stretching vibration at 1000 cm^{-1} and those for the Fe - OH bending at 890 cm^{-1} and 790 cm^{-1} persisted. Evidently, it could be assumed that the bands at 890 cm^{-1} and 790 cm^{-1} were due to structural Fe - OH bending which cannot be affected by digestion in D_2O as long as the initial goethite maintained its structure. In a further study, the evidence for hydroxyl deformations was examined when the phosphated goethites were desorbed by different salts (KCl , KNO_3 , Na_2SO_4) and water. After either 0.1 N KCl solution or water desorption, hydroxyl deformations were not removed in the $1200\text{ cm}^{-1} - 1000\text{ cm}^{-1}$ region. With 0.1 N Na_2SO_4 solution used for desorption, the infrared spectra showed strong

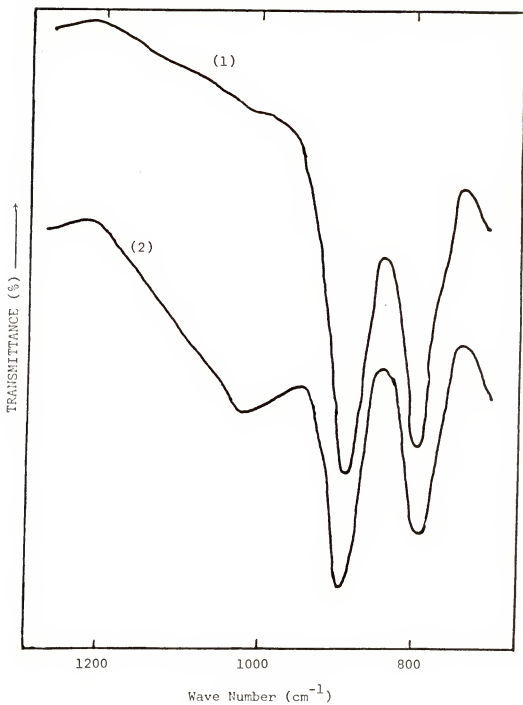


Fig. 12. Infrared bands of 1) goethite digested in D_2O and 2) phosphated goethite digested in D_2O .

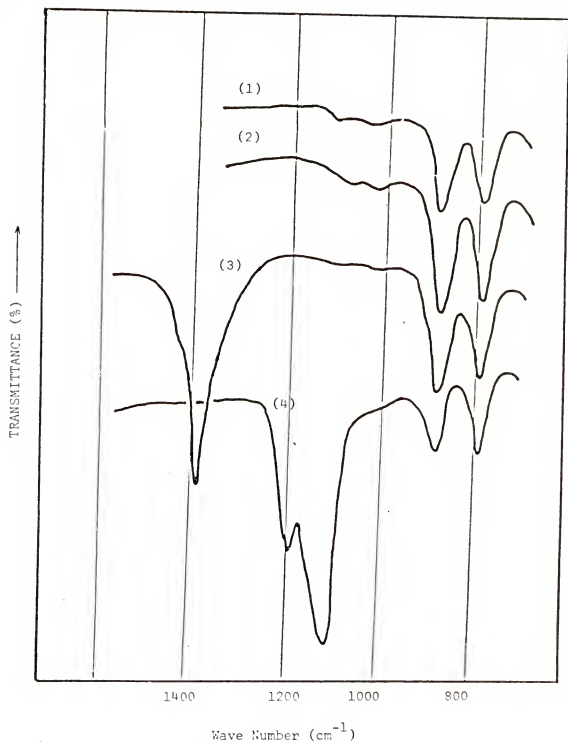


Fig. 13. Infrared bands of phosphated goethite after desorption by (1) 0.1 N KCl, (2) H₂O, (3) 0.1 N KNO₃, (4) 0.1 N Na₂SO₄.

bonds of SO_4^{2-} ions in the $1200 - 1000 \text{ cm}^{-1}$ region. When 0.1 N KNO_3 was used for desorption, NO_3^- appeared to displace some surface phosphates so that the hydroxyl vibration in that region was reduced (Fig. 13). It can be said that NO_3^- and SO_4^{2-} ions have the ability to desorb readily displaceable phosphate at the surface. However, sulfate ions could not be used to provide evidence for this type of phosphate desorption by infrared since sulfate ions have strong vibration in the same region as that of surface-bound phosphate. Parfitt et al. (1975) assigned the appearance of weak bands in the $1200 - 1000 \text{ cm}^{-1}$ region for non-phosphated goethite to the Fe - OH deformational vibration which can partially overlap the region of P = O stretching and P - OH bending vibration.

The question arose about the type of hydroxyl groups that are displaced when phosphates are added to the goethite suspension. Russel et al. (1974) indicated that there were three types of hydroxyl groups: 1) where OH is singly coordinated to an Fe atom with hydrogen bond interaction with another atom, 2) where OH is coordinated to two Fe atoms and 3) when OH is singly coordinated to an Fe atom. Parfitt et al. (1975) considered that only type 3 of OH was displaced by phosphate while OH of the type 1 and 2 are unreactive. The types 1 and 3 of OH, they considered as the structural OH with three vibrations at 3200 , 890 , and 790 cm^{-1} .

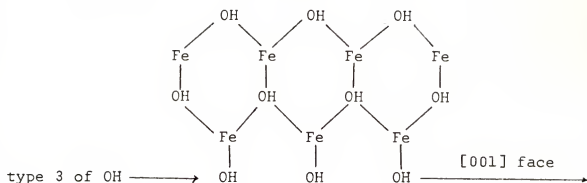


Fig. 14. The 001 face of goethite lattice. (After Bragg and Claringbul 1965).

The formation of binuclear bridging resulted from the displacement of two adjacent type 3 hydroxyls

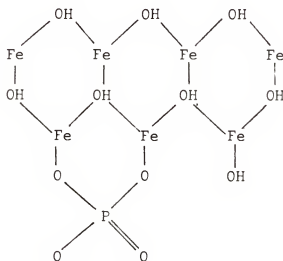


Fig. 15. The 001 face of phosphated goethite.

Phosphate Adsorption and Desorption Studies

Effects of the Initial Concentration

The phosphate adsorption isotherm is obtained by plotting the amount of phosphorus adsorbed ($\mu\text{g P/g}$ of adsorbent)

against the equilibrium concentration of phosphorus in solution. The shape of each isotherm curve is altered by the relative amount of phosphorus adsorbed at each equilibrium concentration and reaction time. For a particular time of adsorption reaction, the amount of phosphorus adsorbed increases with the initial concentration but the percentage of phosphate sorbed decreases.

For the goethite-P solution system, the shapes of the phosphate adsorption isotherm curves were affected by the relative amount of phosphorus adsorbed at each equilibrium concentration (Fig. 16). Each curve was composed of three parts: one at low solute concentration ($< 0.25 \mu\text{g P/ml}$), a second part at higher solute concentration (0.25 to $1.5 \mu\text{g P/ml}$) where the isotherm becomes convex, and a third linear part at higher solute concentration ($> 1.5 \mu\text{g P/ml}$).

However, in the soil-solution system, phosphate adsorptive capacity depended on soil characteristics which affected the shape of the isotherm curves. The Kenya soil and Georgia soil phosphorus sorption curves apparently had two portions, the first part which is a curved portion ($< 5 \mu\text{g P/ml}$) and a second or linear portion ($> 5 \mu\text{g P/ml}$). In Fig. 17, the apparent lack of an initial linear portion for the curve found for Kenya soil suggests need for more adsorption data at low equilibrium concentration ($< 3 \mu\text{g P/ml}$). For the Georgia soil, (Fig. 18), the adsorption maximum is low compared to

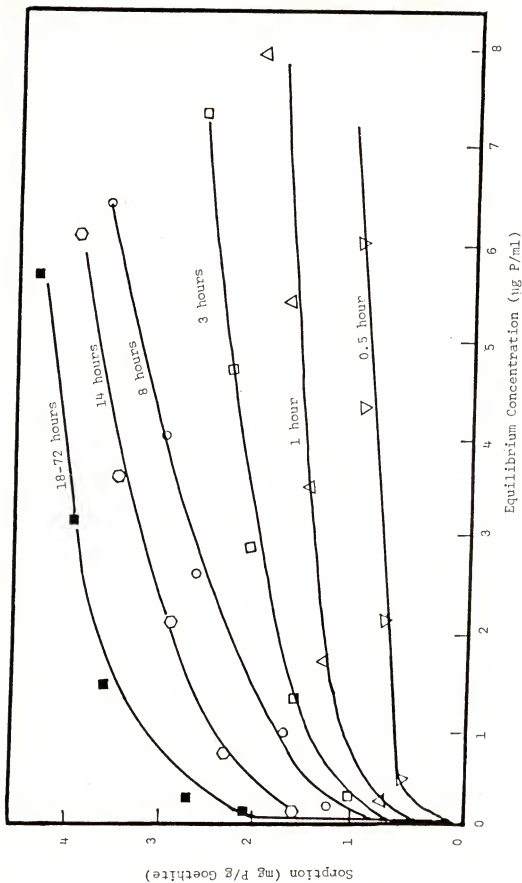


Fig. 16. Adsorption isotherms as affected by the reaction times for goethite-solution systems.

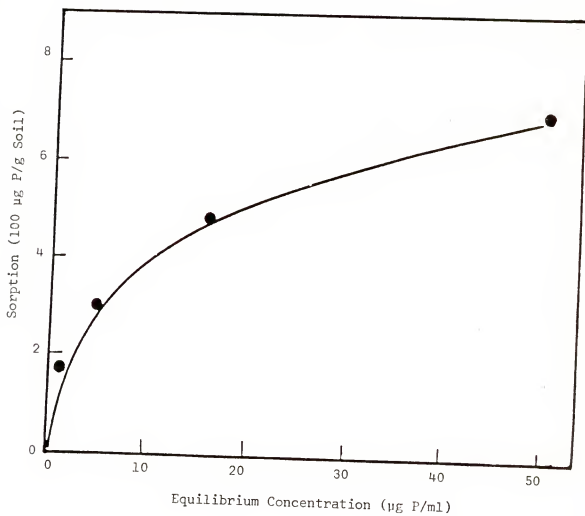


Fig. 17. Adsorption isotherm for the Kenya soil after 24 hours of reaction time.

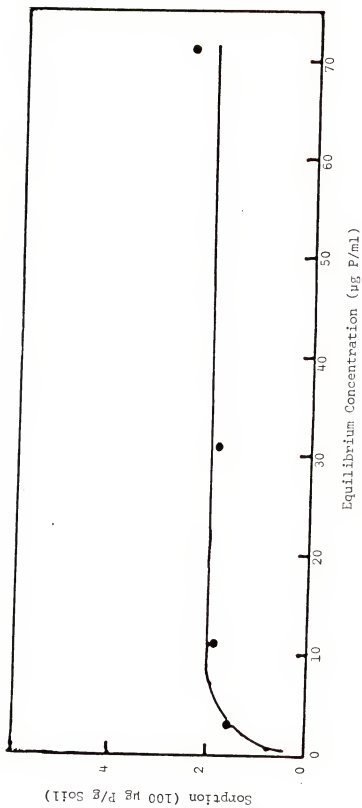


Fig. 18. Adsorption isotherm for the Georgia soil after a reaction time of 24 hours.

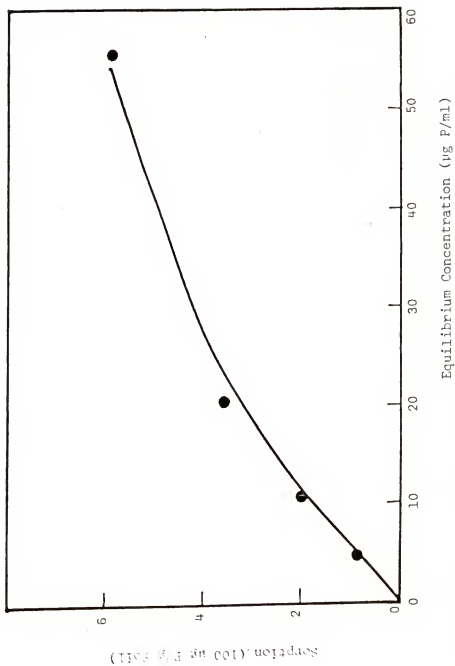


Fig. 19. Phosphate adsorption isotherm for the Colorado soil after 24 hours of reaction time.

that for the Kenya soil, which means that for the same initial concentration in solution more phosphate ions are present in the Georgia soil than in the Kenya soil. For the Colorado soil, (Fig. 19), there is a slight change in slope for the initial and final linear party of the absorption isotherm. For the initial range of equilibrium concentration ranging from 0 to 25 $\mu\text{g P/ml}$, the amount adsorbed increased linearly as the equilibrium concentration increases. This relationship was 20 $\mu\text{g P}$ adsorped per gram of soil for each $\mu\text{g P/ml}$. Muljadi et al. (1966) noted that their isotherm curves were also linear initially with a curved transition to the second linear portion. They ascribed the initial and curved portions to phosphate exchange with OH of $\text{Al}(\text{OH})$ located on the clay edge surfaces. They do not give a clear explanation of the mechanism of adsorption reaction for the third part of the curve but postulated that the final linearity of the isotherm indicated that the number of adsorption sites remained constant even though the amount of phosphate adsorbed increased.

The time required for the reaction to reach equilibrium decreased as the initial concentration decreased, (Fig. 20). If the initial concentration was less than or equal to 5 $\mu\text{g P/ml}$, the steady state of reaction was reached in less than 10 hours. Twenty hours of reaction were required to approach the equilibrium state with an initial concentration

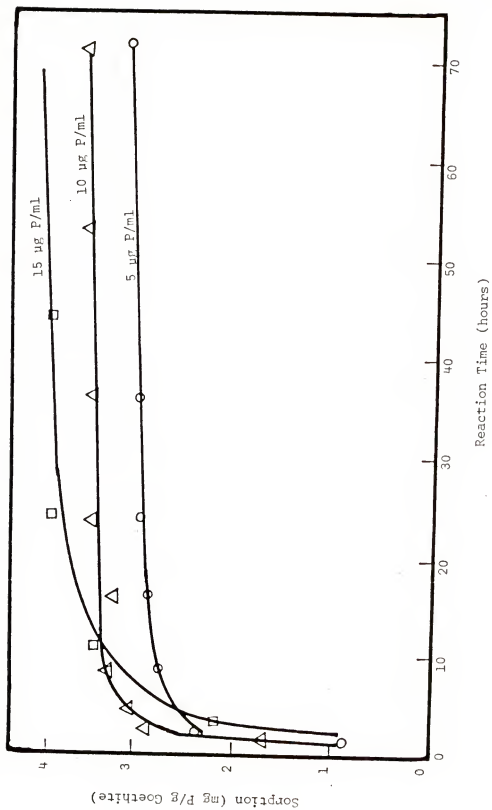


Fig. 20. Effects of the initial P concentration on the phosphate adsorption by goethite-solution (1 g/1000 ml).

greater than or equal to 5 $\mu\text{g P/ml}$. The above observations showed that low amounts of phosphorus were almost instantaneously adsorbed onto the synthetic goethite. Because the initial phosphate potential on the solid phase was low or nil relative to the phosphate potential in solution, the phosphate flux from the solution was therefore high. This movement of phosphate to the solid surface continued for a longer period of time if the initial concentration (or phosphate potential) in solution was high.

Effects of the Supporting Electrolyte

Type of Electrolytes

The adsorption isotherm of phosphate on goethite was examined using molar concentration of the electrolytes, NaCl , CaCl_2 , and AlCl_3 , as given in Fig. 21. Where the initial concentration was greater than 0.5 $\mu\text{g P/ml}$, the salts (electrolyte) gave a significant effect on the amount of phosphorus adsorbed. The adsorption at each concentration decreased in the order $1\text{M } \text{AlCl}_3 > 1\text{M } \text{CaCl}_2 > 1\text{M } \text{NaCl}$. It was noted that the adsorption of phosphate using water as supporting medium gave the same adsorption isotherm as that using 1 $\text{M } \text{NaCl}$ solution. For equilibrium concentration greater than 1 $\mu\text{g P/ml}$, the amount of P sorbed in 1 $\text{M } \text{AlCl}_3$ and 1 $\text{M } \text{CaCl}_2$ was greater than that sorbed in 1 $\text{M } \text{NaCl}$ by a factor of 1.6 and 1.5, respectively.

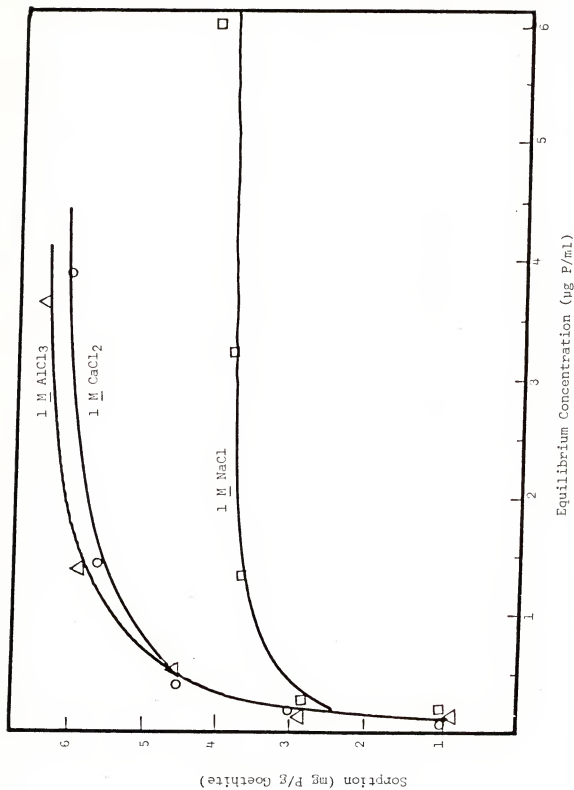


Fig. 21. Effects of the type of supporting electrolyte on P adsorption on goethite-suspension (1 g/1000 ml).

Table 2. Type of salt effects on the P adsorption on goethite at 5 $\mu\text{g P/ml}$.

Electrolyte	P adsorption ($\mu\text{g P/g}$)
1 M NaCl	3780
1 M CaCl_2	5600
1 M AlCl_3	5900

Ryden and Syers (1975) reported that, where some soils have a final concentration above 0.1 $\mu\text{g P/ml}$, the P sorption in 10^{-2} M Ca solution was 1.5 to 2.5 greater than the sorption from water. From the isotherms for P sorption by goethite, the data were arranged as the plots of a/b versus a , where a is the equilibrium concentration, b is the amount of phosphorus adsorbed per unit weight of adsorbent. The linearity of the plots (Fig. 24) confirmed the Langmuir type of adsorbent. When using Eq. (14c) the adsorption maximum (s) and the adsorption energy constant (k) are calculated as shown in Table 3.

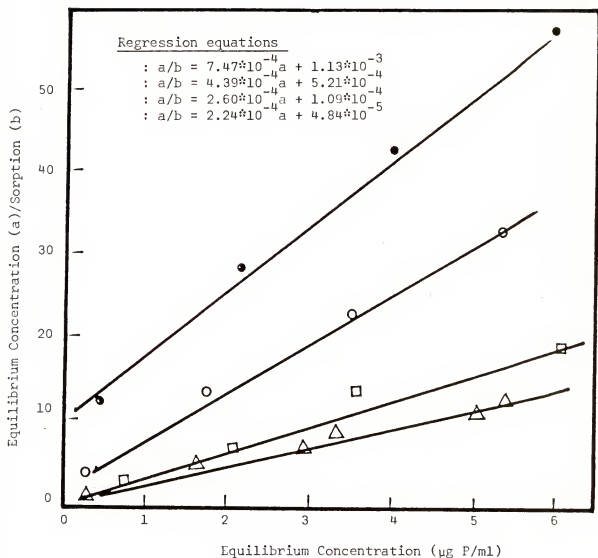
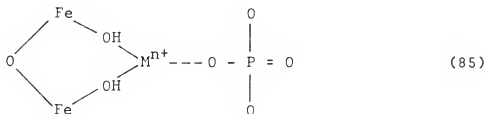


Fig. 24. The transformed Langmuir equations for phosphate sorption by goethite as affected by reaction times. a is equilibrium concentration and b amount adsorbed.

Table 3. Effects of three electrolyte salts on the phosphate sorption maximum and sorption energy constant for goethite.

Electrolyte	Adsorption Maximum	Sorption Energy Constant
	($\mu\text{g P/g}$)	($\text{ml}/\mu\text{g P}$)
1 <u>M</u> NaCl	4300	3.8
1 <u>M</u> CaCl ₂	6900	2.3
1 <u>M</u> AlCl ₃	12700	1.1

The increase of phosphate sorption maximum, (Table 3), was accompanied by a decrease in the apparent sorption energy constant. The increase in phosphate sorption may be due the increase in the cation charge of the electrolyte favored adsorption. A probable way in which the cation charge enters into the phosphate adsorption reaction was through cation bridging:



so that where M is Na, then $n = 0$, or if M is Ca then $n = 1$, and if M is Al then $n = 2$. As the charge on the cation increased, there was a greater attraction between the cation

on the goethite surface and the phosphate ion. The work required to bring the phosphate ion to the cation evidently decreased as the valence increased. The increase in metal valence favored a higher probability that the phosphate was maintained in the goethite-P solution interface, so that the energy for adsorption decreases.

Both aluminum and calcium ions also probably reacted with phosphate in solution to form new phases (precipitation), inducing thereby a decrease of phosphate in solution. Some of the compounds which might precipitate in solution depended both on phosphate concentration (molarity) and pH. These systems can be written as follows:

For CaHPO_4 , the pH and H_2PO_4^- relation is

$$\text{pH}_2\text{PO}_4 = \text{pH} - 3.14 \quad (86)$$

For $\text{Al}(\text{OH})_2\text{H}_2\text{PO}_4$, the pH and H_2PO_4^- relation is

$$\text{pH}_2\text{PO}_4 = \text{pH} + 10.7 \quad (87)$$

For $\text{Fe}(\text{OH})_2\text{H}_2\text{PO}_4$, the pH and H_2PO_4^- relation is

$$\text{pH}_2\text{PO}_4 = \text{pH} - 10.9 \quad (88)$$

The plots of pH_2PO_4 versus pH gave the solubility diagrams of the compounds as illustrated by Lindsay and Moreno (1960). At any point (pH, pH_2PO_4) above the line for a selected compound, precipitation is expected while below the lines dissolution of the corresponding solid phase will occur. In our study, the pH ranged from 6 to 7 so that with

a phosphate concentration of 5 $\mu\text{g P/ml}$ or 1.72×10^{-4} moles of H_2PO_4 per 1 liter, we would have $\text{pH}_2\text{PO}_4 = -\log \text{H}_2\text{PO}_4 = 3.8$; hence, no important amount of precipitation of the above solid phase was expected. Other complex compounds involving combination of Ca and Fe phosphates or Al and Fe phosphates could precipitate near or on colloid surfaces of the goethite or the soils.

Effects of Electrolyte Concentration

Salt concentration had a marked effect on the amount of phosphate sorbed during reactions at various periods. The time at which equilibrium was reached was evidently not affected by increasing the salt concentration (Fig. 22). When the initial concentration is 5 $\mu\text{g P/ml}$, at equilibrium state the phosphate sorption in 1 N CaCl_2 and 0.01 N CaCl_2 is 1.3 and 1.2, respectively, greater than that found for water system without salt. Van Olphen (1977) pointed out that increasing the electrolyte concentration not only caused compression of the diffuse part of the double layer but also some ions, as counter ions, shift from the diffuse layer to the Stern layer. As a result, the ion concentration of the diffuse layer decreased and more adsorption took place. This concept was supported by Ryden and Syers (1975) who found that equilibrium phosphate concentration remained the same in both 10^{-2} M Ca and 10^{-1} M Na systems. Donnan theory could be used to explain the above phenomenon. The inner solution possibly ranged from the solid surface to the

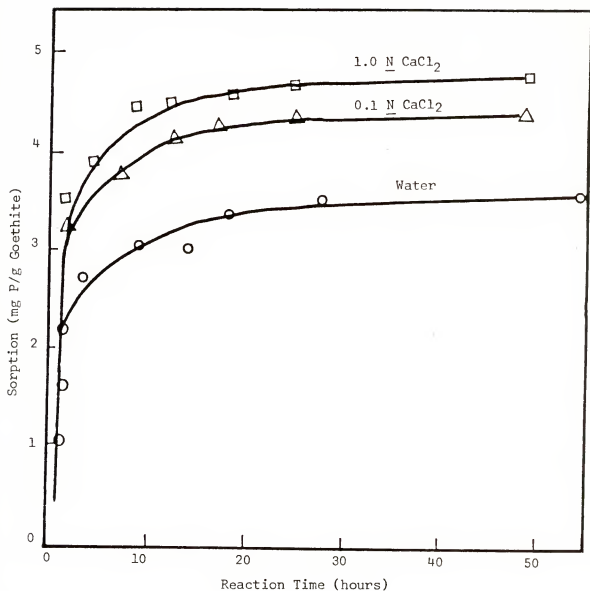


Fig. 22. Effect of the supporting electrolyte concentration on the kinetics of P adsorption by the goethite-solution system (1 g/1000 ml).

Table 4. Phosphate desorption from goethite by different anions.

	Anions (0.1N)					
	Cl ⁻	SO ₄ ²⁻	NO ₃ ⁻	ClO ₄ ⁻	OH ⁻	H ₂ O
% Adsorbed P desorbed	0.3	1.4	1.1	1.3	5.8	2.5

Table 5. Effects of reaction time on phosphate adsorption maximum and sorption energy constant for the goethite system.

Reaction time (hours)	Adsorption Maximum (ug P/g)	Sorption Energy Constant (ml/ug P)
1/10	1340	0.66
1/2	2280	0.84
8	3850	2.40
18 to 76	4460	4.60

Table 6. The logarithm of (a) equilibrium P concentration as a function of the logarithm of (b) amount of P adsorbed.

	log a			
	-.45	.15	3.07	5.54
log b	3.40	3.55	3.60	3.65

imaginary limit of the physically adsorbed ions and the outer solution containing all free ions. This could be expressed as:

$$(M)^{1/n}(H_2PO_4)_O = (M)_i^{1/n}(H_2PO_4)_i = k \quad (89)$$

where $(M)_O$ and $(M)_i$ are the concentrations of the cation M of valence n in the outer solution and inner solution respectively, terms $(H_2PO_4)_O$ and $(H_2PO_4)_i$ are the phosphate concentrations in the outer and inner solutions, respectively, and k is a constant. From the above equation, it was evident that as salt concentration $(M)_O$ increased, the $(H_2PO_4)_O$ concentration must decrease. As a result, phosphate may be adsorbed through cation bridging or precipitation as cation-phosphates.

Phosphate Desorption

Effects of phosphate free solutions of 1 M $AlCl_3$, and $CaCl_2$ and NaCl are shown in Fig. 23. There was a significant effect of the type of salt on the extent of phosphate desorption. The magnitude of differences due to salt sources increased as the equilibrium phosphate concentration increased. For a low equilibrium concentration (1 μg P/ml), the desorption with 1 M $AlCl_3$ solution released 550 μg P/g of goethite. This was 3.1 and 1.8 times greater than similar desorption by 1 M $CaCl_2$ and 1 M NaCl, respectively. The higher desorption of phosphate by 1 M $AlCl_3$ solution agreed with the apparent lower potential binding energy constant of

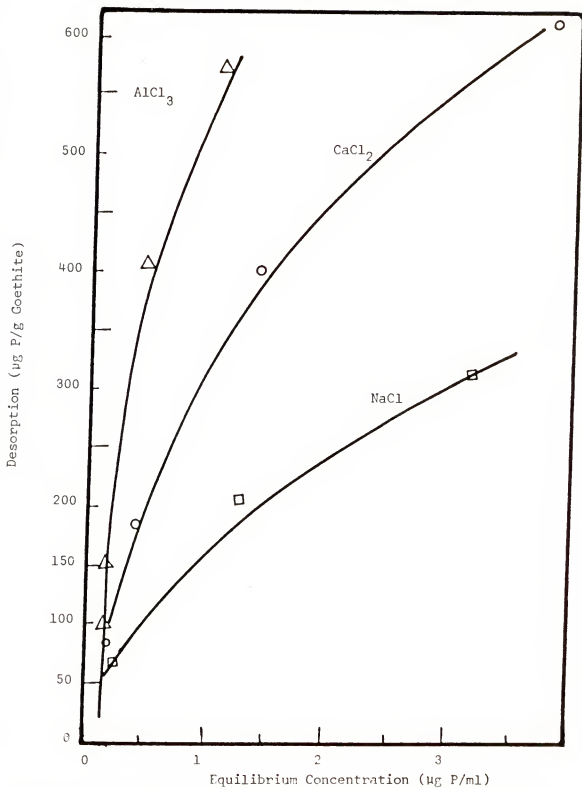


Fig. 23. Phosphate desorption in 10 hours from goethite by three salt solutions at various equilibrium P concentration.

phosphate in goethite-P solution in the presence of this salt. The increase in phosphate adsorption due to increase of cation valence was also accompanied by an increase in the desorbed fraction which was weakly bound (Fig. 23). This would suggest that the additional phosphate adsorption in presence of multivalent cations may not only be due to direct surface binding but also to other bonding by some form of cation bridging and/or multilayer phosphate adsorption. These latter forms were easily replaced during P desorption with further fresh salt solutions.

Time of Reaction Effects

Adsorption Reaction

From the decrease in the initial phosphate concentration, the phosphate sorption increased with time and remained constant when the reaction time was greater than 18 hours for goethite-P solution system (Fig. 25). The adsorption made according to the transformed Langmuir equation, Eq. (14c), was linear. This suggest that the surface of the synthetic goethite was composed of an homogeneous population of sites for the adsorption of phosphate. In Fig. 24, it can be seen that both the slope and intercept of the sorption isotherms decreased as the reaction time increased up to 18 hours. In Table 5 it was shown that both the calculated adsorption maximum and the potential binding energy constant

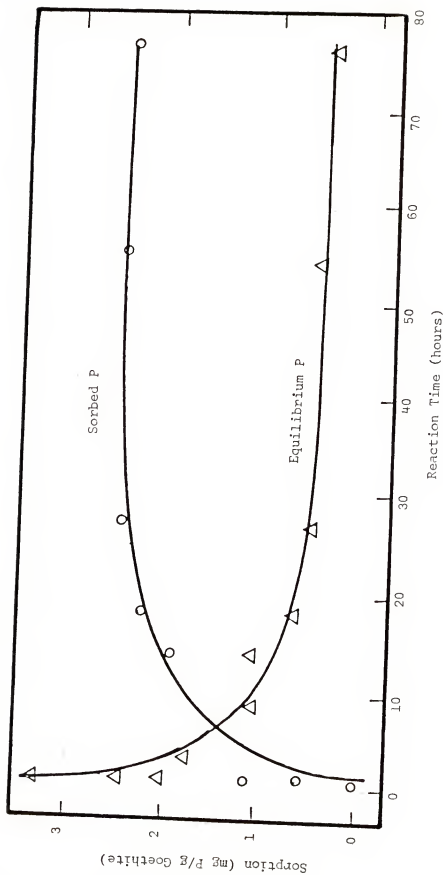


Fig. 25. Change in the equilibrium P concentration and P sorption by goethite as affected by the reaction time.

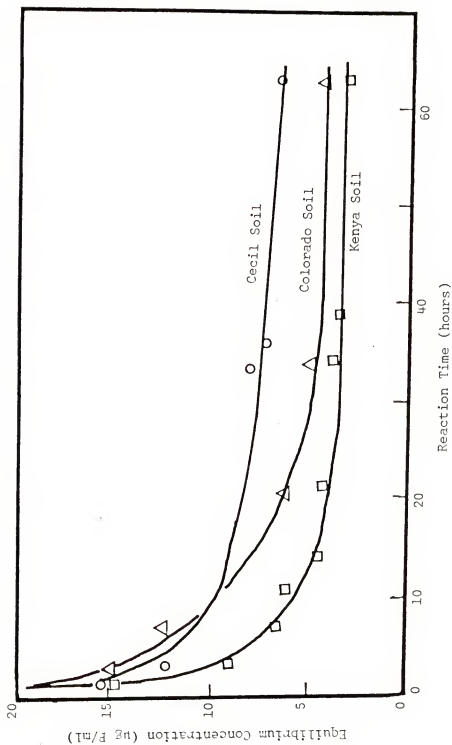


Fig. 26. Change in the equilibrium P concentration for three soils as affected by the reaction times.

increased as the reaction time increased. Changes in this potential binding energy constant increased as the reaction time increased. Changes in this potential binding energy might be explained by the fact that as the surface becomes covered by phosphate, further adsorption of other phosphate ions occurred on the remaining free surface which required much more energy for bonding than on the first monolayer (Clark 1970). It should be kept in mind that the Langmuir equation assumed that there was only a monolayer of adsorbed P and that there was no lateral interaction between the adsorbed ions. As a result, the application of the Langmuir equation to experimental data would require that the reaction time be specified since the nature of the adsorbed layer would not be defined with time.

The increase of energy constant as the adsorption maximum increases was not in disagreement with studies by Aharoni and Ungarish (1977) who stated that adsorption took place in the initial stages on the sites with lowest energy at a particular time. When comparing materials of different mineralogical composition, Ryden and Syers (1975) found that consistent trend for increase in the energy constant with the adsorption maximum confirmed the assumption that phosphate was usually adsorbed onto all available low energy sites before the high energy sites were filled. In the present studies, using the P sorption data for goethite-P

solution when the reaction times exceeded 18 hours, further treatment of the data was made using the transformed Freundlich relationship given in Eq. (10). From Table 7, the plot of $\log a$ versus $\log b$ was close to linearity as the following regression equation:

$$\log b = 0.209 \log a + 3.50 \quad (90)$$

Therefore, the free energy of adsorption (expressed as the energy difference between the adsorbed and free state of phosphate) decreased exponentially as the binding energy and surface coverage increased.

From the proposed kinetic model given in Eq. (57) and Eq. (59b), an attempt was made to predict the change with respect to time that occurred for forms of phosphate logically in the system. These were (A) free ions such as H_2PO_4^- , (B) the physically and reversible chemically adsorbed phosphate, and (C) the irreversible chemically adsorbed phosphate. A transformation of Eq. (57a) can be written as

$$\ln a = w_1(t - t_0) + k \quad (91)$$

where a is the equilibrium concentration, w_1 and k are constant, t is the reaction time, and t_0 is the equilibrium time equal to 18 hours. According to the sorption, data were plotted using Eq. (91) and are given in Fig. 30. It can be seen that the phosphate adsorption reaction on goethite followed two steps before the equilibrium was reached. The first step was finished after 3 hours of reaction time (t_1),

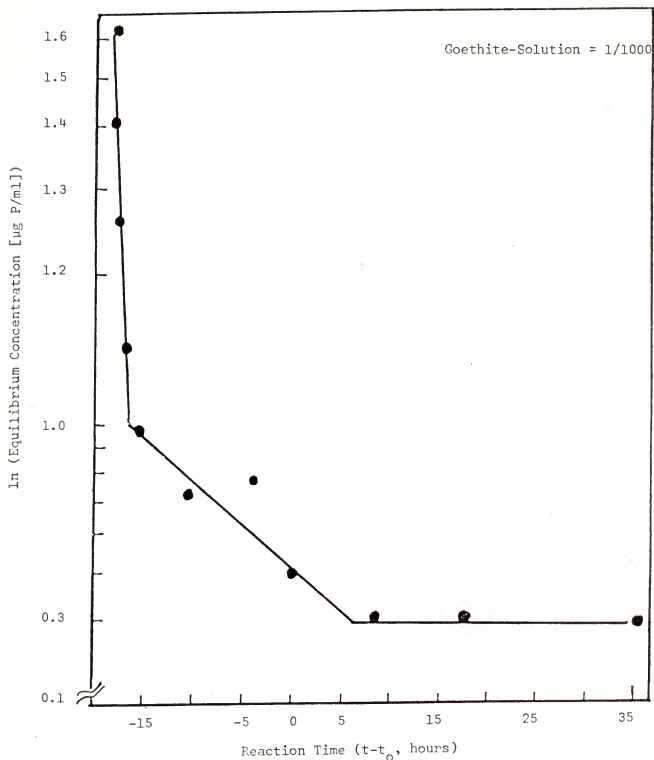


Fig. 30. Logarithmic plot of equilibrium P concentration change with time (t) relative to equilibrium at 18 hours (t_0) for phosphated goethite. Data were obtained using Eq. (91).

and the second step after 3 to 18 hours (t_0). From these data it was apparent that Eq. (57a) should be split into two components with respect to time after initiating the experiment so that

$$a_1 = a_{0e} w_{1a}(t - t_0) \quad (92a)$$

and for the range t_1 to t_0

$$a_2 = a_{01e} w_{1b}(t - t_0) \quad (92b)$$

so that a_1 is the initial P concentration in solution for $t \leq t_1$ and a_2 is the solution P concentration at longer reaction time between t_1 and t_0 . In the goethite-P solution system, there was an initial fast reaction so that $w_{1a} = 0.133 \text{ hour}^{-1}$ and a second step of the reaction which was slower with $w_{1b} = 0.025 \text{ hour}^{-1}$. This would also apply for the fast and slow adsorption reactions observed by Barrow and Shaw (1975).

Desorption of Phosphate

After the phosphate adsorption was conducted for different periods of time, the desorption curve shown in Fig. 27 for the Kenya soil indicated that the phosphate desorption in 0.01 \underline{M} CaCl_2 was almost linear with respect to P concentration in the equilibrium solution and that the adsorption reaction time affected the desorption process. With an initial concentration of 20 $\mu\text{g P/ml}$ after 23 hours

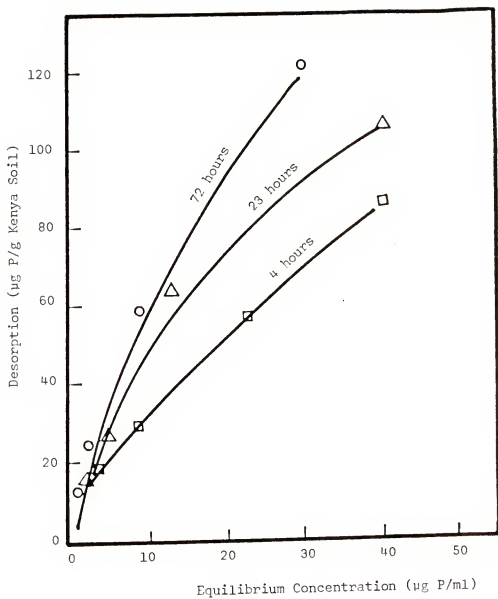


Fig. 27. Effect of reaction time and equilibrium P concentration on P desorbed by 0.01 N $CaCl_2$ from Kenya soil.

of adsorption reactions in 0.01 N CaCl_2 solution desorption was 80 $\mu\text{g P/g}$ for Kenya soil. Similarly at each equilibrium concentration, the desorption of phosphate increased for the Georgia soil. Fig. 28 also showed more desorption of P from the Colorado soil after 23 hours of P adsorption than that after 27 hours. For the Colorado soil, the phosphate desorption data indicate that if the equilibrium concentration was greater than 5 $\mu\text{g P/ml}$, there was a divergence in phosphate release as the adsorption reaction time increased. In Fig. 29 extraction with 0.5 N NH_4F at pH3.8 resulted in a significant increase in phosphate release, presumably from that in aluminum form. Apparently, more phosphate was held as an aluminum phosphate after 72 hours of adsorption than after 21 hours, a negligible amount being recovered after 4 hours of adsorption time. This might explain the lower desorption of phosphate by 0.01 N CaCl_2 at longer adsorption time.

In the goethite-P solution system, (Fig. 25), phosphate adsorption at first increased and then remained constant as the reaction time was increased. This indicated that there is first a predominant physically adsorbed P followed by a conversion to chemically adsorbed P; this is supported by the increase in P sorption energy constant (Table 5). The free phosphate will replace some of the physically adsorbed phosphate until a stable layer will be established and the system is then at equilibrium.

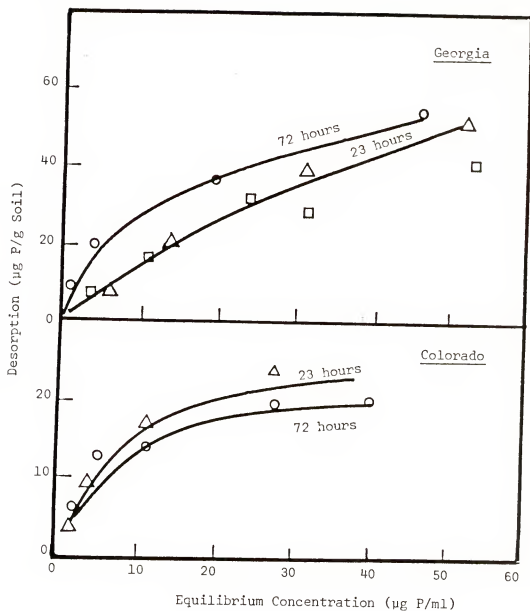


Fig. 28. Effect of reaction time and equilibrium F concentration on P desorbed by 0.01 N CaCl_2 from the Georgia and Colorado soils.

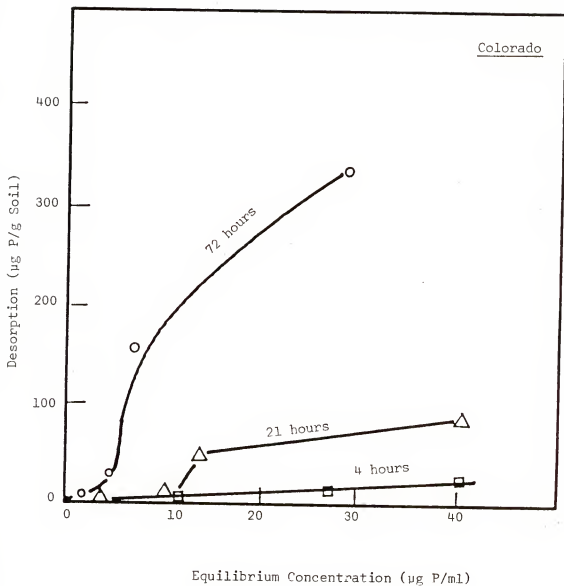


Fig. 29. Effect on P desorbed by $0.5\text{ N NH}_4\text{F}$ as affected by the adsorption reaction time and equilibrium P concentration.

Effects of pH on P Adsorption and Desorption

Adsorption

The adsorption of phosphates both on goethite and soils induced an increase in the equilibrium solution pH, (Table 7). The calculated pH change was 0.75×10^{-5} pH units/ $\mu\text{g P/g}$ of goethite in the soil-P solution systems; it was 3.75×10^{-3} , 2.14×10^{-3} , and 0.75×10^{-3} pH units per $\mu\text{g P/g}$ soil for the Georgia, Kenya, and Colorado soils, respectively. In the goethite-P solution studies, phosphate adsorption increased with decreasing pH of the equilibrium solution (Fig. 31). When the initial P solution was 5 $\mu\text{g P/ml}$, the amount of phosphate adsorbed decreased almost linearly with pH of the equilibrium solution was increased according to the equation

$$(\mu\text{g P/g}) = -446 \text{ pH} + 5680 \quad (93)$$

where P is the amount of P absorbed on goethite.

The effects of pH on the prevalence of the orthophosphate species in solution have been investigated. From Lindsay and Vlek (1977), each of the following phosphate species constituted more than 50% of the total P at the following respective pH range: i) H_3PO_4 for pH 2 or less, ii) H_2PO_4^- for pH 2 to 7, iii) HPO_4^{2-} for pH 7 to 12, and iv) PO_4^{3-} for pH greater than 12. Such changes in phosphate ions with pH further complicated the interpretation of phosphate adsorption. As the pH increased, the goethite had an increasing net negative charge (Eq. 64). Since the

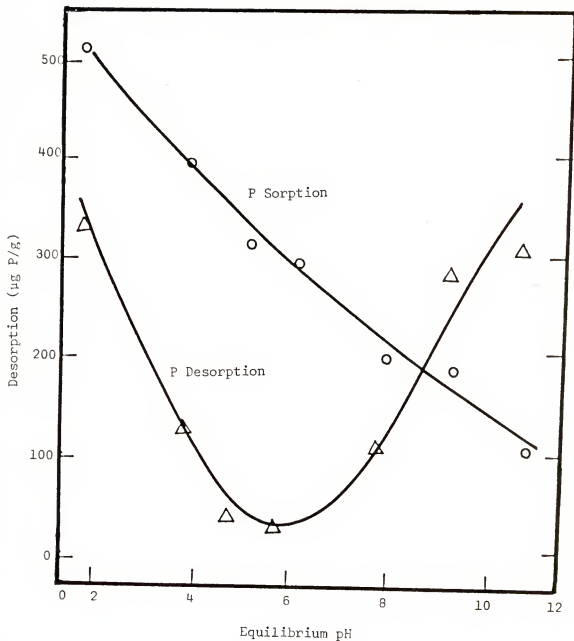


Fig. 31. Effect of change in equilibrium solution pH on P adsorption and 0.01 N CaCl_2 desorption of P in goethite system. Initial P concentration is 5 $\mu\text{g/ml}$.

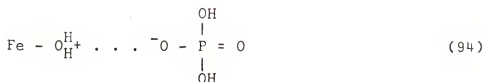
Table 7. Effects of P adsorption on the equilibrium solution pH after 24 hours of adsorption reaction.

Adsorbent	P added ($\mu\text{g P/g}$)	P adsorbed ($\mu\text{g P/g}$)	pH	
			Initial	Final
Goethite	5	3500	7.10	7.30
	10	4300	6.60	7.00
Georgia	5	179	5.10	5.55
	10	202	5.10	5.47
Colorado	5	198	6.80	7.03
	10	374	6.57	6.69
Kenya	5	304	5.50	6.06
	10	490	5.40	5.95

predominant orthophosphate ions are in the increasing order H_2PO_4^- , HPO_4^{2-} , PO_4^{3-} with increasing pH, from the electrostatic point of view, there was an increasing repulsion between the goethite surface and the orthophosphate ions. This resulted in less phosphate adsorbed with an increase in pH. Hingston et al. (1967) found that the maximum adsorption of goethite was approached when the pH was less than 4. At such low pH, goethite would have a net positive surface and phosphate ion would be negatively charged. As a result, minimum repulsion or maximum attraction between goethite surface and phosphate ions should occur at this acidity.

Desorption

The reversibility of the adsorbed phosphates from solution at different pH condition is shown in Fig. 31. The pH at which the phosphate adsorption took place had an important effect on the reversibility of phosphate adsorption. As the pH of the equilibrium solution (adsorption process) increased, there was first a decrease in the quantity of phosphate desorbed until a minimum was reached in the range pH 5 to pH 6 followed by decreased desorption as pH was further increased. At less than pH 5, both phosphate adsorption and desorption were greatly increased. This indicated that, as the pH decreased, there were some additional positive sites formed on the goethite surface. One probability was the shift of hydronium ion to the hydroxyl group of Fe - OH as shown below



resulting in more phosphate adsorption. However, when the pH was greater than 6, there was an increase in the hydroxyl ion concentration which has strong affinity for any positive site. Consequently, the existence of competition between OH^- and the orthophosphate ions for the same type of sites resulted in lower phosphate adsorption. Hingston et al. (1968) noticed that anions were desorbed by competitive effect when the competitor can occupy sites in addition to those already occupied by other anions, hence the increase in the negative charge of the surface. This increase in negative charge produced by the competitor allowed phosphate desorption by surface hydroxyls. It was known that the increase in OH^- concentration favored the formation of surface negative sites, which contribute to the weak phosphate binding resulting in greater P desorption.

The competitive capacity of hydroxyl for phosphate sites was further confirmed from data shown in Fig. 32. The pH effect on the equilibrium P concentration after various adsorption times was markedly different for pH2 and pH10. At pH2, the desorption of phosphate increased initially and remained constant after 5 hours of reaction time. However at pH10 the phosphate desorption increased sharply initially

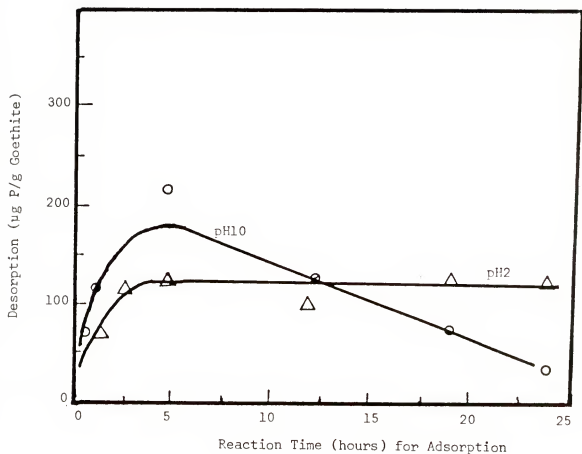


Fig. 32. Effect of phosphate adsorption time on phosphate desorption by 0.01 N CaCl_2 at pH 2 and pH 10.

and thereafter decreased slowly and linearly as the reaction time increases. This shows that at pH 10 the hydroxyls ions continued the phosphate desorption as the adsorption reaction time was increased. This apparent increase in efficiency for OH replacement of phosphate might also have included calcium phosphate precipitation as well as the fact that much of the phosphate ions were probably in trivalent state. Obviously, ageing of the phosphated goethite negated phosphate desorption by OH replacement.

Effects of pH and Time

In order to define the response of phosphates desorption with time and pH, the desorption was conducted at both different periods of time and pH. From the data shown in Fig. 33, at both 6 and 12 hours of desorption time, phosphate desorption followed the same pattern over the same pH range. However, after 20 minutes, only at pH 10 was substantial amounts of phosphate desorbed (600 $\mu\text{g P/g}$ goethite) which is about 1/3 of the amount that was obtained after 12 hours of desorption at this pH. Generally, it can be said that the efficiency of phosphate desorption increased as the pH of the desorbing solution was increased.

The effects of the electrolyte concentration and pH interaction on phosphate desorption are shown in Fig. 34. The phosphate desorption at any pH increased when supporting electrolyte was present compared to use of water only for

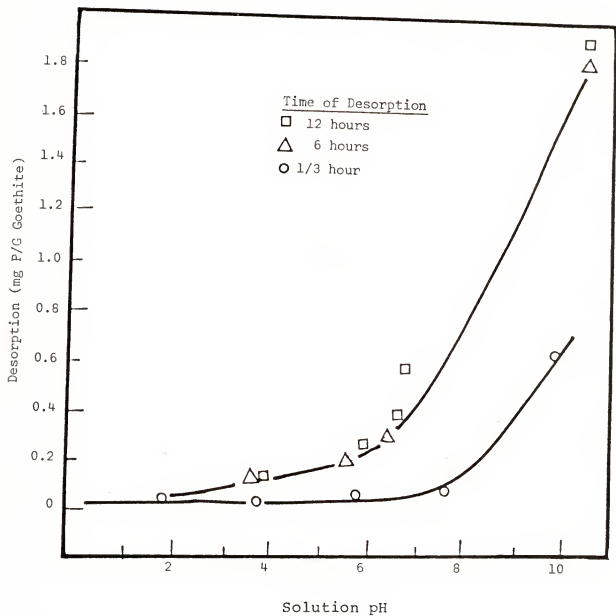


Fig. 33. Effects of solution pH on the amount of P desorped from goethite.

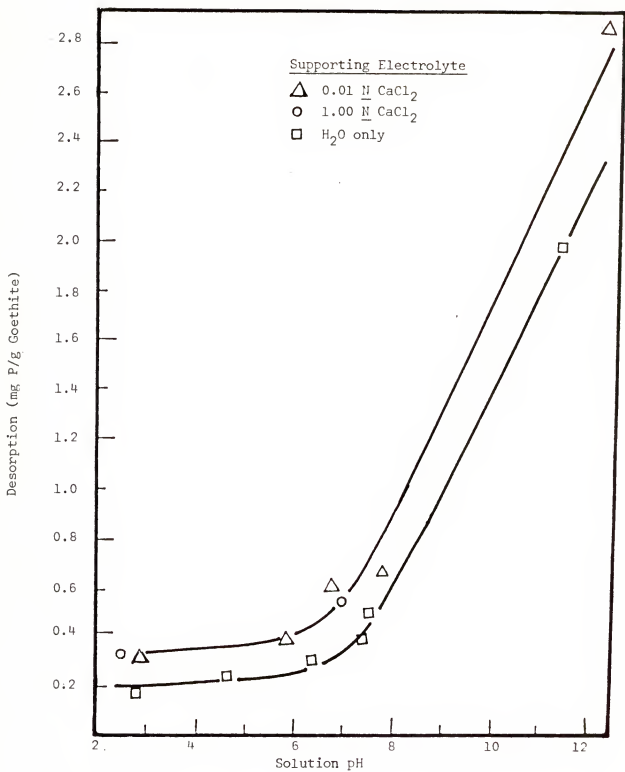


Fig. 34. Effects of pH and concentration of supporting electrolyte on phosphate desorption.

phosphate desorption. In the range pH 2 to pH 12, either 1 N CaCl_2 or 0.01 N CaCl_2 gave similar amounts of desorption phosphate at each pH, and each is greater than that obtained from water. At any pH, the phosphate desorption in 0.01 N CaCl_2 was approximately 200 $\mu\text{g P/g}$ goethite greater than the amount desorbed in water.

Effects of P Adsorption on Surface Charge of Goethite

In goethite-solution and soil solution system, it was assumed that H^+ and OH^- ions are potential determining ions. Potentiometric titration of goethite was made to determine the zero point of charge (ZPC) from the distribution of the net electric charges with varying pH and electrolyte concentrations (Fig. 35). The ZPC was at the inflexion point of the titration curves at different electrolyte concentrations. Parfitt and Atkinson (1976) reported a decrease of the pH for ZPC from 8.1 to 5.1 as a result of the adsorption of 100 μmole of NaH_2PO_4 on goethite. According to Mekaru and Uehara (1972), each millimole of P sorbed increased the CEC by approximately 0.8 meq at pH 7 on some ferruginous tropical soils. In this study, when using synthetic goethite, ZPC was at pH 5.8 for goethite (shown in Fig. 36), compared to ZPC at pH 5.2 for phosphated goethite (as a result of 3000 $\mu\text{g P}$ adsorbed per g goethite). From Eq. (66) it was deduced from Gouy-Chapman theory that there should be an increase in negativity as a result of phosphate adsorption. In the

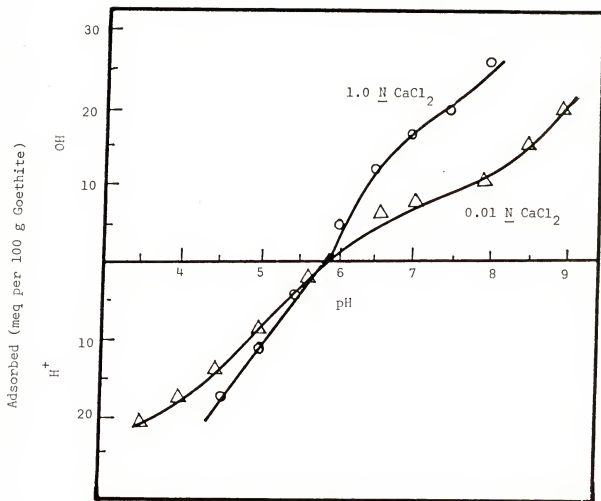


Fig. 35. Potentiometric titration of goethite. Note zero point of charge occurs at pH 5.8.

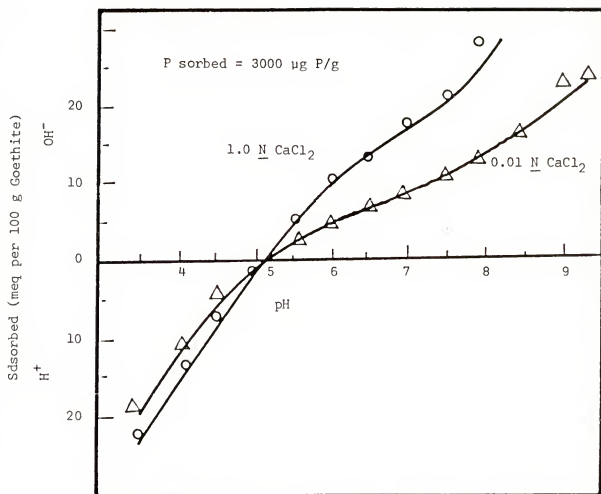


Fig. 36. Potentiometric titration of phosphated goethite.
Not zero point of charge occurs at pH 5.2.

present study, the goethite was freed of electrolyte by dialysis prior to ZPC determinations. This process may have had some effect on the nature of the goethite surface since loosely bound ions were removed in the process. In a soil system, all surfaces have various cations and anions present on the clay surfaces which affect both phosphate adsorption-desorption and ion activities resulting after phosphate adsorption. From the present studies, both pH and electrolyte changes greatly affected the degree of phosphate desorption.

CHAPTER VI SUMMARY AND CONCLUSION

The low availability of phosphate ions in tropical soils is of major concern to all workers recognizing the need to increase agricultural production. In this study, conditions favoring the formation of iron oxyhydroxides such as goethite were investigated. An attempt was made to understand the mechanism through which phosphate may be bound to goethite using infrared spectroscopy. Using goethite and/or soils as supporting medium, the influence of some factors on the kinetics of phosphate adsorption and desorption were studied.

The conditions for goethite preparation were investigated. Goethite was made by mixing FeCl_3 and NaOH solutions and allowing the precipitates to crystallize. The identification of the presence of goethite in the suspension was made by infrared spectroscopy supported by X-ray diffraction. The infrared spectra indicated that the bands characteristic of goethite formation are at 3200 cm^{-1} (Fe - OH stretching), 890 cm^{-1} and 790 cm^{-1} (which are both Fe -OH bending vibrations). The appearance of 2.19 \AA and 2.70 \AA peaks from the X-ray diffraction also was supporting evidence that most of the components resulting from mixtures with $\text{OH/Fe} = 6$ were

goethite. Both the speed and the degree of goethite crystallization increased as the OH/Fe ratio was increased. This was seen through the increase in the above band intensities. From this study, goethite was not a major component in a suspension of OH/Fe = 1.5 which was aged only for 50 hours, as reported by some workers. With OH/Fe = 1.5 in the suspension, there was need both to age for a longer period of time and to increase the temperature of the suspension to increase the formation of Fe - OH bonding.

The presence of phosphate at the beginning of the ageing process weakened the structure of goethite. From the data found experimentally, evidence of competition existed between the phosphate and the hydroxyl ions for bonding with iron. The increase of phosphate concentration in the suspension ($P/Fe = 0.032$ to 3.2) induced more and more the formation of the P - O(Fe) bonds as seen by the 1000 cm^{-1} vibrations. The surface adsorption of phosphate on goethite was identified through the appearance of vibrational bands in the $1200 - 1000\text{ cm}^{-1}$ region. The appearance of hydroxyl deformation in the same region was also identified by treatment of the phosphated goethite with D_2O . However, it was believed that the bands at 1160 , 1085 , and 1030 cm^{-1} for phosphated goethites were characteristic of phosphate binuclear bridging, $(FeO)_2POOH$. The existence of such type of binding is further confirmed by the increase of negative

surface charge, or decrease of the point of zero charge after the phosphate adsorption.

Using synthetic goethite, phosphate adsorption and desorption were affected by the initial concentration, the supporting electrolyte, the reaction time, and pH of the system. The amount of phosphate adsorbed was proportional to the initial phosphate concentration. In goethite-solution system (1 g/1000 ml), maximum phosphate adsorption was reached when the initial solute concentration was at least 10 $\mu\text{g P/ml}$. The calculated adsorption maximum, according to the Langmuir equation, increased in each case with time, the electrolyte concentration, and the valence of the cation. Increase in phosphate adsorption resulted from an increase in salt concentration. This was also accompanied by a substantial increase in phosphate desorbed by water. The increase in phosphate adsorption due to increasing cation valence was also accompanied by an increase in phosphate desorption by the water in the corresponding electrolyte over that for water only. The addition of cations might have contributed to the phosphate adsorption either through cation bridging or to a multilayer of physically adsorbed phosphate. This was supported by the fact that an increase of cation valence was not accompanied by an increase of the apparent sorption energy constant. Only with time was the phosphate adsorption reaction accompanied by an increasing

sorption energy constant. Changing of the goethite suspension and phosphate systems from pH 2 to pH 12 resulted in a change in phosphate adsorption because there was competition between the hydroxyl and phosphate ions for adsorption sites. The adsorption decreased almost in a linear fashion as the pH increased. At the same initial equilibrium P concentration, the phosphate desorption was reduced when the adsorption solution pH was less than 6; but when the pH was greater than 6 the desorption phosphate increased. This showed that more phosphate was displaced from the chemically adsorbed forms to desorbable forms. This phosphate desorption increased with time up to 6 hours and remained constant from 6 to 12 hours.

Both Langmuir and Freundlich equations were used to describe the relationship between the amount of phosphorus absorbed and the equilibrium concentration in goethite and soils systems. Since those equations were valid only at a particular reaction time, a kinetic model was proposed to describe the change of ions in solution as the reaction time increased. The model fractionated phosphate absorption change with time for the physically adsorbed and reversible chemically adsorbed phosphate ions compared to that for the irreversible chemically adsorbed phosphate. From the proposed kinetic model, an expression for minimum energy for irreversible fixation was deduced. The experimental data showed

that before the equilibrium state was reached, the adsorption reaction proceeded through two essentially linear-type reactions with respect to the reaction time.

The phosphate adsorption isotherm for soils indicated no major differences from those of other workers. The Kenya soil had the highest adsorption compared to that of a Colorado soil and a Georgia soil. Phosphate adsorption reached the equilibrium state after 22 to 24 hours of reaction time. For any initial concentration greater than 5 $\mu\text{g P/ml}$, desorption of phosphate by 0.01 N CaCl_2 solution increased with the absorption reaction time for goethite and for the Kenya and Georgia soils, but not for the Colorado soil. This desorption was in agreement with the fact that after phosphate desorption by 0.01 N CaCl_2 , further phosphate extracted by the 0.5 $\text{N NH}_4\text{F}$ increased as the adsorption reaction time increased. Some of the phosphate adsorption at shorter time periods was extractable by 0.01 N CaCl_2 , but at longer adsorption reaction periods, phosphate bonding strength increased.

Some of the factors determining the phenomena of adsorption-desorption have been investigated. In order to relate these studies to phosphate fertilization of tropical soils and phosphate adsorption-desorption reaction, such studies conducted in the laboratory should be complemented by pot studies involving tropical plants. Later, from these

findings, field experiments would be necessary to provide demonstration plots on advances in technology for phosphorus fertilization of tropical soils.

LITERATURE CITED

- Aharoni, C., and M. Ungarish. 1977. Kinetics of activated chemisorption. *J. Chem. Soc. Faraday Trans I.* 73:1943-1950.
- Atkins, P. W. 1978. *Physical chemistry.* p. 192. Freeman Company. San Francisco.
- Atkinson, R. J., R. L. Parfitt and R. C. Smart. 1974. Infrared study of phosphate adsorption on goethite. *J. Chem. Soc. Faraday. Trans. I* 70:1472-1479.
- Atkinson, R. J., A. M. Posner, and J. P. Quirk. 1968. Crystal nucleation in Fe(III) solutions and hydroxide gels. *J. Inorg. Nucl. Chem.* 30:2371-2381.
- Bach, B. W., and E. G. Williams. 1971. A phosphate sorption index for soil. *J. Soil Sci.* 22:289-301.
- Baldwin, J. P., P. H. T. Nye, and P. B. Tinker. 1973. Uptake of solutes by multiple root systems from soils. III A model for calculating the solute uptake by a randomly dispersed root system developing in a finite volume of soil. *Plant and Soil* 38:621-635.
- Ballard, R. 1974. Extractability of reference phosphates by soil test reagents in absence and presence of soils. *Soil and Crop Soc. Sci. Fla. Proc.* 33:169-174.
- Barrow, N. J., P. G. Ozanne, and T. C. Shaw. 1965. Nutrient potential and capacity. *Aust. J. Agric. Res.* 16:61-76.
- Barrow, N. J., and T. C. Shaw. 1975. The slow reactions between soil and anions: 2. Effect of time and temperature on P concentration in solution. *Soil Sci.* 119:167-177.
- Beckett, P. H. T. 1971. Potassium potentials. *Fot. Rev. Subj.* 5, 30:1-41.
- Beckett, P. H. T., and R. E. White. 1964. Studies on the phosphate potentials of soils. Part III. The pool of labile inorganic phosphate. *Plant and Soil* 21:251-281.

- Bolt, G. H. 1976. Soil Chemistry. A. Basic elements. p. 43-44. Elsevier Scientific. Publ. Co., Amsterdam.
- Bragg, L. and G. F. Claringbull. 1965. The crystal structure of minerals, Bell Publishing Co., London.
- Brunauer, S. 1943. The adsorption of gases and vapors. Vol I. Physical adsorption, p. 196-217, Princeton Univ. Press.
- Busca, G., N. Cotena, and P. F. Rossi. 1972. Infrared spectroscopic study of micronised goethite. Mater. Chem. 3:271-284.
- Clark, A. 1970. The theory of adsorption and catalysis. P.258. Academic Press, New York and London.
- Colthup, N. B., L. H. Daly, and S. E. Wiberley. 1975. Introduction to infrared and raman spectroscopy. 2nd ed. Acad. Press., New York.
- de Camargo, O. A., J. W. Biggar, and D. R. Nielson. 1979. Transport of inorganic phosphorus in an Alfisol. Soil Sci. Soc. Amer. Proc. 43:884-890.
- Digiand, F. A., G. B. B. Frick, and H. Sontheimer. 1978. A simplified competitive equilibrium adsorption model. Chem. Eng. Sci. 53:1667-1673.
- Eying, A. H. and E. M. Eying. 1963. Modern chemical kinetics. p. 10-13. Reinhold Publ. Co. New York.
- Farmer, V. C. and F. Palmieri. 1975. The characterization of soil minerals by infrared spectra. p. 573. In Soil components V2, Giesecking (ed.), Springer-Verlag, New York.
- Ghani, M. O. and M. A. Islam. 1946. Phosphate fixation in acid soil and its mechanism. Soil Sci. 62:293-306.
- Haseman, J. F., E. H. Brown, and C. D. Whitt. 1950. Reaction of phosphate with clay and hydrous oxide of iron and aluminum. Soil Sci. 70:257-271.
- Hemwall, J. B. 1957. Phosphorus fixation. Adv. Agron. J:95-112.
- Hingston, F. J., R. J. Atkinson, A. M. Posner, and J. P. Quirk. 1967. Specific adsorption of anions. Nature, 215:1459-1461.

- Hingston, F. J., R. J. Atkinson, A. M. Posner, and J. P. Quirk. 1968. Anion adsorption by goethite and gibbsite. I the role of the proton in determining adsorption envelopes. *J. Soil Sci.* 23:177-191.
- Hingston, F. J., A. M. Posner, and J. K. Quirk. 1974. Anion adsorption by goethite and gibbsite. II Desorption of anions from hydrous oxide surfaces. *J. Soil Sci.* 25:16-26.
- Holford, I. C. R., and G. E. G. Mattingly. 1975. Phosphate sorption by Jurassic oolitic limestones. *Geoderma*, 13:257-264.
- Hsu, P. H. 1965. Fixation of phosphate by Al and Fe in acidic soils. *Soil Sci.* 99:398-402.
- Hsu, P. H. 1972. Nucleation polymerization and precipitation of FeOOH . *J. Soil Sci.* 23:409-419.
- Jaroniec, M. and J. Toth. 1976. Adsorption of gas mixtures on heterogeneous solid surfaces. *Coll. and Poly. Sci.* 254:643-649.
- Jossen, L., J. M. Prausnitz, W. Fritz, E. U. Schlunder, and A. L. Myers. 1978. Thermodynamic of multi-solute adsorption from dilute aqueous solutions. *Chem. Eng. Sci.* 33:1097-1106.
- Keng, J. C. M., and G. Uehara. 1974. Chemistry mineralogy and taxonomy of oxides and ultisols *Soil Sci. Soc. Amer. Proc.* 33:119-126.
- Kiselev, A. V., and V. I. Lygin. 1975. Infra-red spectra of surface compounds. p. 60. John Wiley and sons, New York.
- Kuo, S., and E. G. Lotse. 1972. Kinetics of phosphate adsorption by Ca-carbonate and Ca-kaolinite. *Soil Sci. Soc. Am. Proc.* 36:725-729.
- Laverdiere, M. R. and R. M. Weaver. 1977. Change characteristics of spodic horizons. *Soil Sci Soc. Amer. Proc.* 41:505-510.
- Lindsay, W. L., and E. C. Moreno. 1960. Phosphate phase equilibrium in soil. *Soil Sci. Soc. Amer. Proc.* 24:177-182.

- Lindsay, W. L. and P. L. G. Vlek. 1977. Phosphate minerals. p. 639. In minerals in soil environments. Soil Soc. Sci. Amer. Madison, Wis.
- Lingstrom, F. T., L. Barsma, and H. Gardina. 1968. 2, 4D diffusion in saturated soils: A mathematical theory. Soil Sci. 106:107-113.
- Lingstrom, F. T., R. Haque, and W. R. Coshaw. 1970. Adsorption from solute. III A new model for the kinetics of adsorption-desorption processes. J. Phys. Chem. 74:495-502.
- Mekaru, T., and G. Uehara. 1972. Anion adsorption in ferruginous tropical soils. Soil Sci Soc. Amer. Proc. 36:296-309.
- Muljadi, D., A. M. Posner, and J. P. Quirk 1966 The mechanisms of P adsorption by kaolinite, gibbsite and pseudo-baehmite. Part I isotherms and effect of pH on adsorption. J. Soil Sci 17:213-227.
- Murphy, P. H., A. M. Posner and J. P. Quirk 1975 Chemistry of iron in soils. Ferric hydrolysis products. Aust. J. Soil Res. 13:189-201.
- Nakamoto, K. 1978 Infrared and raman spectra of inorganic and coordination compounds. 3rd ed. John Wiley and Sons, New York.
- Parfitt, R. L. 1979. The nature of the phosphate goethite (α -FeOOH) complex formed with $\text{Ca}(\text{H}_2\text{PO}_4)_2$ at different surface coverage. Soil Soc. Amer. Proc. 43:623-625.
- Parfitt, R. L., and R. J. Atkinson. 1976. Phosphate adsorption on goethite (α -FeOOH). Nature. 264:740-742.
- Parfitt, R. L., R. J. Atkinson, and R. C. Smart 1975 The mechanism of phosphate fixation by Iron oxides. Soil Sci. Soc. Amer. Proc. 39:837-841.
- Parks, G. A. and P. L. de Bruyn. 1962. The zero point of charge of oxides J. Phys. Chem. 66:967-972.
- Peterson, G. W. and R. B. Corey. 1966. A modified Chang and Jackson procedure for routine fractionation of inorganic soil phosphates. Soil Sci. Soc. Amer. Proc. 30:563-565.

- Russel, J. D., R. L. Parfitt, A. R. Fraser, and V. C. Farmer. 1974. Surface structures of gibbsite and phosphated goethite. *Nature* 248:220-221.
- Ryden, J. C. and J. K. Syers. 1975. Rationalization of ionic strength and cation effects on phosphate sorption by soils. *J. Soil Sci.* 26:395-406.
- Schwertman, U., and R. M. Taylor. 1977. Non oxides. M. J. B. Dixon (ed). *Minerals in soil environments*, p 145-180, Soil Soc. Amer., Madison, Wis.
- Schofield, R. K. 1955. Can a precise meaning be given to available soil phosphorus. *Soil and Fertilizers*, 28:373-375.
- Sennett P. and J. P. Olivier. 1965. Colloid dispersion, electronic effects and the concept of zeta potential. *Amer. Chem. Soc.* 57:32-50.
- Soil investigation staff. 1972. Soil survey laboratory methods. U.S. Dept. Agr. report No. 1.
- Syers, J. K., M. G. Brauman, G. W. Smillie, and R. B. Corey. 1973. Phosphate sorption by soils evaluated by the Langmuir adsorption equation. *Soil Sci. Soc. Amer. Proc.* 37:358-364.
- van Olphen, H. 1977. An introduction to clay colloid chemistry for clay technologists, geologists and soil scientists. 2nd ed., John Wiley and Son, New York.
- Vlad, M., and E. Segal. 1979. Generalization of the Jaroniec isotherm. *Surf. Sci.* 79:608-616.
- Yuan, T. L., W. K. Robertson, and J. R. Weller. 1960. Forms of newly fixed phosphorus in three acid sandy soils. *Soil. Sci. Soc. Amer. Proc.* 24:447-450.

BIOGRAPHICAL SKETCH

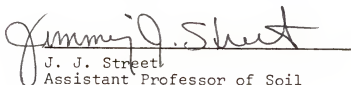
Yekini Bourahim was born on December 13, 1948 in Dakar (Sénégal). He completed his high school education at Lycée Technique Coulibaly of Cotonou (Benin) where he obtained the degree Baccalauréat (mathématique) in 1970. He immediately entered the Institut National Agronomique de Tunis and obtained after four years his Ingénieur Agricole degree. He then entered the Université Nationale du Benin and obtained his Ingenieur Agronome (Science du Sol) degree in 1976. He served for one year as Assistant Professor at the Université Nationale du Benin. He entered the University of Florida (Soil Science department) in 1977, and he is currently a Ph.D. degree candidate.

I certify that I have read this study and that in my opinion it conforms to acceptable standards of scholarly presentation and is fully adequate, in scope and quality, as a thesis for the degree of Doctor of Philosophy.



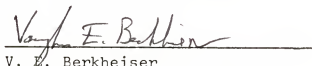
John G. A. Fiskell, Chairman
Professor of Soil Science

I certify that I have read this study and that in my opinion it conforms to acceptable standards of scholarly presentation and is fully adequate, in scope and quality, as a thesis for the degree of Doctor of Philosophy.



J. J. Street
Assistant Professor of Soil
Science

I certify that I have read this study and that in my opinion it conforms to acceptable standards of scholarly presentation and is fully adequate, in scope and quality, as a thesis for the degree of Doctor of Philosophy.




V. E. Berkheiser
Assistant Professor of Soil
Science

I certify that I have read this study and that in my opinion it conforms to acceptable standards of scholarly presentation and is fully adequate, in scope and quality, as a thesis for the degree of Doctor of Philosophy.



W. K. Robertson
Professor of Soil Science


I certify that I have read this study and that in my opinion it conforms to acceptable standards of scholarly presentation and is fully adequate, in scope and quality, as a thesis for the degree of Doctor of Philosophy.



R. C. Stoufer
Associate Professor of Chemistry

This dissertation was submitted to the Graduate Faculty of the College of Agriculture and to the Graduate Council, and was accepted as partial fulfillment of the requirements for the degree of Doctor of Philosophy.

June 1980



Dean, College of Agriculture

Dean, Graduate School